ACTIVE CONTROL OF THE FORCED AND TRANSIENT RESPONSE OF A FINITE BEAM

By

John Theodore Post

B.S.E.E., May 1987, University of Arkansas

A Thesis submitted to

The Faculty of

The Graduate School of Engineering and Applied Science of
The George Washington University in partial satisfaction
of the requirements for the degree of Master of Science

20 October, 1989

Abstract

When studying structural vibrations resulting from a concentrated source, many structures may be modelled as a finite beam excited by a point source. This research explores the theoretical limit on cancelling the resulting beam vibrations by utilizing another point source as an active controller. Three different types of excitation are considered, harmonic, random, and transient. In each case, a cost function is defined and minimized for numerous parameter variations.

For the case of harmonic excitation, the cost function is obtained by integrating the mean squared displacement over a region of the beam in which control is desired. A controller is then found to minimize this cost function in the control interval. The control interval and controller location are continuously varied for several frequencies of excitation. The results show that control over the entire beam length is possible only when the excitation frequency is near a resonant frequency of the beam, but control over a subregion may be obtained even between resonant frequencies at the cost of increasing the vibration outside of the control region.

For random excitation, the cost function is realized by integrating the expected value of the displacement squared over the interval of the beam in which control is desired. This is shown to yield the identical cost function as obtained by integrating the cost function for harmonic excitation over all excitation frequencies. As a result, it is always possible to reduce the cost function for random excitation whether controlling the entire beam or just a subregion, without ever increasing the vibration outside the region in which control is desired.

The last type of excitation considered is a single, transient pulse. A cost function representative of the beam vibration is obtained by integrating the transient displacement squared over a region of the beam and over all time. The form of the controller is chosen a priori as either one or two delayed pulses. Delays constrain the controller to be causal. The best possible control is then examined while varying the region of control and the controller location. It is found that control is always possible using either one or two control pulses. The two pulse controller gives better performance than a single pulse controller, but the effort to find the optimal delay time for each additional controller pulse increases as the square of the number of control pulses.

Acknowledgements

I would like to express my most sincere thanks to those who have assisted me during the preparation of this thesis. Thanks to the Structural Acoustics Branch (SAB) at NASA/Langley Research Center for sponsoring this research and to my SAB advisor, Mr. Richard J. Silcox, for his effort in overseeing my work. Thanks to my thesis advisor, Dr. Michael K. Myers, who has taught me more than he suspects. Also, without the kind assistance and seemingly endless patience of Dr. Jay Hardin and Dr. Feri Farassat, the theoretical developments would not have been possible.

I would like to extend a special thanks to the many wonderful people I have meet at NASA, especially those in the Acoustics Division, who made my stay more enjoyable. Finally, I would like to thank my friends and family, because it is their loving support which gives me the strength to succeed.

Table of Contents

Table of Figures

Figure | Page

Table of Tables

Table of Symbols

E	Young's modulus
$f_s(t)$	force of excitation source
$f_c(t)$	controlling force
$h(t)$	impulse response of controller
$h_c(x,t)$	response of beam due to impulsive force at controller location, x_c
$h_s(x,t)$	response of beam due to impulsive force at source location, x_s
$H_c(x,\omega)$	Fourier transform of $h_c(x,t)$
$H_s(x,\omega)$	Fourier transform of $h_s(x,t)$
$H(s)$	Laplace transform of $h(t)$
$H(\omega)$	Fourier transform of $h(t)$
i,k,m,n	integers
I	area moment of inertia
j	$\sqrt{-1}$
l	length of beam
$\bar{m}$	mass per unit length
$R_f(\tau)$	autocorrelation of $f(t)$ at lag τ
t	time
T_n	period of eigenfrequency ω_n, equal to $2/(n^2\pi)$
$u_s(t)$	Heaviside unit step function
α	time delay between successive control pulses
δ_{mn}	Kronecker delta function

$\delta(t)$	Dirac delta function
δ	variation
$\delta_t h(x,t)$	variation of function $h(x,t)$ with respect to t.
Δ	discrete time step
ζ_n	viscous damping coefficient of nth beam mode
Λ	cost function representing the beam vibration for transient excitation, equal to the transient displacement squared, integrated over all time and some beam length
σ_f^2	variance of $f(t)$
$\phi_n(x)$	nth beam mode (eigenfunction), equal to $\sin n\pi x$
Φ	cost function representing the beam vibration for harmonic excitation, equal to the mean squared value of harmonic displacement integrated over some beam length
Ψ	cost function representing the beam vibration for random excitation, equal to the expected value of displacement squared integrated over some beam length
ω	radian frequency
ω_n	natural frequency of nth beam mode
$\omega_{d,n}$	damped resonant frequency of nth beam mode, equal to $\omega_n\sqrt{1-\zeta_n^2}$
F^*	complex conjugate of variable F
$\Re$	denotes real part of a complex quantity
$\bar{y}$	time average of variable y.
$\hat{y}$	the complex amplitude of a real quantity y which is harmonic with frequency ω, defined such that $y(t) = \Re\{\hat{y}e^{j\omega t}\}$
$< >$	represents expected value of enclosed variables
$\angle$	denotes phase angle of complex quantity

Chapter 1

INTRODUCTION

With our increasing involvement in the area of aerospace technologies, the need to control large, flexible aerospace structures such as aircraft, space stations, radio telescopes, or solar energy panels grows more important. Unwanted vibrations in these structures may result in poor instrument performance, noisy interiors, or even structural failure.

Traditional methods for controlling unwanted vibrations in a structure used passive isolators or stiffened the structure such that it became more difficult to excite. Passive isolators are useful only over a small frequency band because they are tuned for a single frequency. Isolators also give poor performance at low frequencies. Adding stiffness to the structure results in increased weight. The design of aerospace vehicles is extremely sensitive to weight.

A novel approach to control, made possible by advances in the digital computer, is active control. This method utilizes additional sources of disturbance to cancel out the undesired disturbance. Suppressing vibration in resonating structures by active control techniques is receiving extensive study[1-6]. The plausibility of actively controlling a structure modelled as a linear system has been confirmed[7,8]. Very often, the structure to be controlled may be modelled as a beam. It may be desired to control the flow of energy through the beam or the vibration of the beam itself depending on the application. In an infinite or semi-infinite domain, the flow of energy in the

beam is the quantity to be controlled. For a finite domain, controlling the vibration of the beam itself becomes the problem. This thesis is concerned with controlling the vibration of a finite beam.

If the beam is connecting some mechanical device to a supporting structure, vibrations propagate through the beam into the structure. This is a situation in which it is suitable to control the flow of energy through the beam in an effort to isolate it from the structure without concern for the vibration of the beam itself. It has been demonstrated that this flexural power flow in beams modelled as infinite or semi-infinite can be attenuated with a small number of actuators[9-12].

For finite systems, control is desired over some spatial region. Balas[13] describes a method for applying active control to distributed structures and demonstrates the method with an example for a simply-supported beam. The equation of motion for an undamped beam in bending is solved by the method of eigenfunctions. This information is incorporated in a linear control system, in which information from a sensor is used to estimate the modal amplitudes and velocities. The steady-state controller produces control proportional to the modal amplitudes by minimizing a performance function via a single actuator. The first three modes of the system after control are found to be positively damped for the case of a transient excitation. Meirovitch and Baruh[14] also control a simply-supported beam using a concept referred to as Independent Modal-Space Control (IMSC). In this method, the modes of the beam are controlled independently, so that one is effectively controlling a set of independent second-order systems in parallel. This allows for a relatively simple design and quick implementation for real time control. The drawback to IMSC is that an actuator is necessary for each mode to be

controlled, and in some cases, the number of these can be quite large. The large number of actuators makes the control system more expensive and may cause design conflicts arising from positioning the actuators. Meirovitch and Silverberg[15] demonstrate an application of IMSC by modeling an aircraft wing as a cantilever beam and controlling the flutter modes excited by a constant velocity airflow.

All of the studies described above in the area of beam control use some scheme to observe the motion of the beam which allows the actuator to implement the appropriate control. The sensor provides feedback to the actuator so that the vibrating beam is controlled without regard to the input disturbance and the actuator continues to damp out the vibrations in the beam after the source of disturbance has been discontinued. This thesis is concerned with the best theoretical control possible, assuming complete knowledge of the beam's mechanics a priori via the beam equation, and does not require any scheme to estimate the state of the system. Since the eigenvalues and eigenvectors of the beam are assumed to be known, the only additional knowledge that is needed for establishing optimal control of the beam is any restrictions on the controller and the input excitation.

Three different cases of input excitation from a point source on the beam are considered, and the resulting vibration is controlled by a second point source linearly related to the excitation source. It is this linear relation, hereafter referred to as the controller, that is sought such as to give the best control possible.

First the excitation is assumed to be steady-state sinusoidal. A measure of control is defined by integrating the mean square displacement over some length of the beam. The controller that best minimizes this quantity is then

found and its performance demonstrated. The best controller is acausal but because the excitation is sinusoidal and therefore completely predictable under steady-state conditions, causality is not a constraint for this controller. It is referred to as the unconstrained harmonic controller.

For the second case the beam excitation is assumed to be a stationary, white-noise random process. The cost function minimized for this case is obtained by integrating the expected value of the displacement squared over some length of the beam. The controller that best minimizes this quantity is then found and its performance demonstrated. This controller is referred to as the unconstrained random controller.

The last type of excitation controlled is not a steady-state excitation as in the case of the previous controllers sought, but a single, transient impulse. The form of the controller is chosen a priori as either one or two delayed, independent impulses. The delay time and weight of the control pulses are chosen such as to minimize the squared displacement response integrated over time and some beam length.

When the best controllers have been found for the previously mentioned types of excitation, the results are compared for different configurations. The controller location and the interval of control are varied as well the frequency in the harmonic case.

Chapter 2

SOLUTION TO BEAM EQUATION

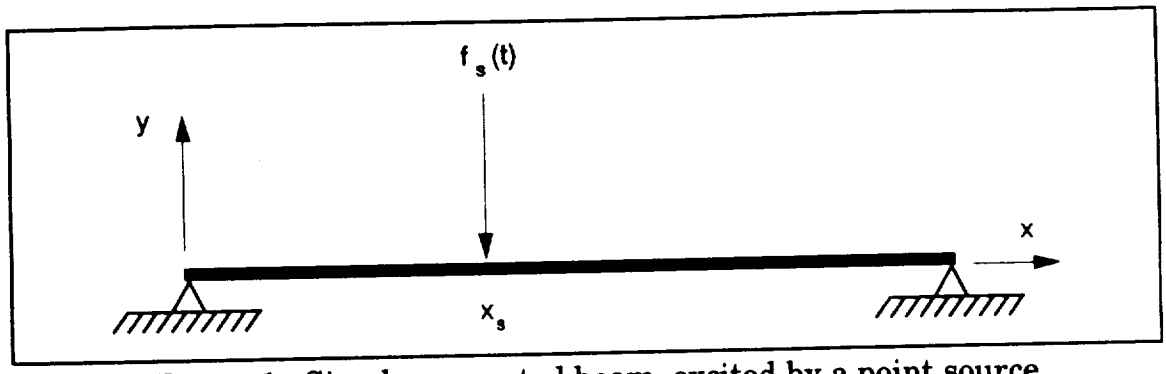

Figure 1. Simply supported beam, excited by a point source

In this chapter, the equations governing the vibration of a beam are developed. The following chapters will use this theory when adding a control force to minimize the vibration in the beam. Since the beam equation is linear, only one point force need be used in developing the equations of motion. Additional point forces are handled by superposition of solutions.

Given the simply supported, Bernoulli-Euler[16] beam in Figure 1, the governing equation for small, transverse vibrations is

$$\bar{m}\frac{\partial^2 y(x,t)}{\partial t^2} + EI\frac{\partial^4 y(x,t)}{\partial x^4} = f(x,t) \tag{1}$$

with $0 \le x \le l$ and $0 \le t$. The bending stiffness is EI, $\bar{m}$ the linear mass density, and f(x,t) the distributed force loading. It is convenient to nondimensionalize equation (1) by utilizing the following dimensionless variables for space and time:

$$x = \frac{\mathrm{x}}{l} \qquad \text{and} \qquad t = \sqrt{\frac{EI}{\bar{m}l^4}}\mathrm{t} \tag{1.1}$$

Now equation (1) becomes

$$\frac{\partial^2 y(x,t)}{\partial t^2} + \frac{\partial^4 y(x,t)}{\partial x^4} = f(x,t) \tag{1.2}$$

where $0 \le x \le 1$, $0 \le t$ and $f(x,t)$ is a nondimensional loading force given by

$$f(x,t) = \frac{l^4}{EI}\mathrm{f(x,t)} \tag{1.3}$$

For the point force shown in Figure 1, and throughout this thesis $f(x,t) = f_s(t)\delta(x_s)$. The simply supported beam is subject to the following boundary conditions:

$$y(0,t) = y(1,t) = 0 \tag{2}$$

$$\frac{\partial^2 y(0,t)}{\partial x^2} = \frac{\partial^2 y(1,t)}{\partial x^2} = 0 \tag{3}$$

Equation (2) fixes the ends of the beam while equation (3) ensures that the ends of the beam are free to rotate by requiring zero applied moment.

The homogeneous equation of (1.2) can be solved to find the natural vibration frequencies and associated beam modes or eigenfunctions[17]:

$$\omega_n = (n\pi)^2 \qquad n = 1,2,3,\ldots \tag{4}$$

$$\phi_n(x) = \sin n\pi x \qquad n = 1,2,3,\ldots \tag{5}$$

The particular or "forced" solution can be obtained using the method of eigenfunctions. Assume an expansion of the displacement in the form

$$y(x,t) = \sum_{n=1}^{\infty} \phi_n(x) y_n(t) \tag{6}$$

where the generalized coordinate $y_n(t)$ for the nth beam mode is to be determined. Substituting equation (6) into (1) and using the orthogonality of the beam modes results in the following second-order uncoupled equations after adding a modal viscous damping term ζ_n :

$$\frac{d^2y_n(t)}{dt^2} + 2\omega_n\zeta_n\frac{dy_n(t)}{dt} + \omega_n^2 y_n(t) = 2\phi_n(x_s)f_s(t) \tag{12}$$

Adding the damping at this point may seem unconventional, but it is a common step in the structural field[16]. Putting a damping term in equation (1) would only serve to complicate finding the eigenvalues for the beam. A small damping term is included here to prevent an infinite response of the beam at resonance. In practice the actual modal damping value ζ_n is almost always determined experimentally[18].

Equation (12) can be solved to give

$$y_n(t) = 2\phi_n(x_s)\int_0^t d\tau\, h_n(\tau)f_s(t-\tau) \tag{13}$$

where

$$h_n(t) = \frac{1}{\omega_{d,n}}e^{-\omega_n\zeta_n t}\sin\omega_{d,n}t\, u_s(t) \tag{14}$$

and

$$\omega_{d,n} = \omega_n\sqrt{1-\zeta_n^2} \tag{15}$$

The function $h_n(t)$ is the impulse response of the nth beam mode and $u_s(t)$ is the Heaviside function. Now with equations (6) and (13) the general solution for the steady-state beam displacement can be written as a convolution between the exciting force and the impulse response of the beam:

$$y(x,t) = \int_0^\infty d\tau\, h_s(x,\tau)f_s(t-\tau) \tag{17}$$

where $$h_s(x,\tau) = 2\sum_{n=1}^{\infty} h_n(\tau)\phi_n(x_s)\phi_n(x) \tag{18}$$

The impulse response function $h_s(x,\tau)$ is by definition the response of the beam at position x due to an impulsive force at position x_s at time $\tau = 0$.

For the case of harmonic excitation, let the force be represented by

$$f_s(t) = \Re\{\hat{f}_s e^{j\omega t}\} \tag{19}$$

where $\hat{f}_s$ is in general complex and $\Re$ denotes the real part of a complex quantity. In harmonic analysis the system is assumed to be in its steady-state. In the steady-state, all quantities are oscillating at the same frequency ω, so all have representations similar to the exciting force in equation (19). For simplicity, only the complex amplitudes (indicated by a hat) will be utilized in the analysis, and it is understood that the physical quantities are found by multiplying by $e^{j\omega t}$ and taking the real part.

Substitute equation (19) into (17) to give

$$y(x,t) = \int_{-\infty}^{\infty} d\tau\, h_s(x,\tau)\Re\{f_s e^{j\omega(t-\tau)}\}$$

Now it can be seen that

$$\hat{y}(x,\omega) = H_s(x,\omega)\hat{f}_s \tag{20}$$

where $H_s(\omega)$ is the Fourier transform[19] of the impulse response of the beam.

The Fourier transform pair is defined by

$$H(\omega) = \int_{-\infty}^{\infty} dt\, h(t)e^{-j\omega t} \tag{21.1}$$

$$h(t) = \frac{1}{2\pi}\int_{-\infty}^{\infty} d\omega H(\omega)e^{j\omega t} \tag{21.2}$$

Fourier transforming equation (18) and (14) gives

$$H_s(x,\omega) = 2\sum_{n=1}^{\infty} \phi_n(x_s)\phi_n(x)H_n(\omega) \tag{22}$$

where

$$H_n(\omega) = \frac{1}{\omega_n^2 - \omega^2 + 2j\omega\omega_n\zeta_n} \tag{23}$$

Equation (22) gives the transfer function between the displacement of any point on the beam and the exciting force. Figure 2 shows this transfer function for the displacement at $x = 1/6$ due to an exciting force at $x_s = 1/6$ for the first 3 modes. The damping was taken to be 1%. The response of the modes is well separated and very peaked since the damping is small. The phase shift of π radians below and above the resonance frequencies is expected. Note the phase change of π between the first and second modes. This phase change marks the frequency at which the displacement of the beam due to the response of the second mode dominates the displacement due to the first mode.

The closed form solution to the beam equation found in this chapter will be used throughout the remaining analysis in this thesis. It is worthwhile to point out, though, that the remaining analysis is not only applicable to a simply supported finite beam. The eigenfunctions and eigenvalues of more complicated systems can be found numerically by computer programs such as NASTRAN, and utilized in the same manner as those of the beam found in this chapter.

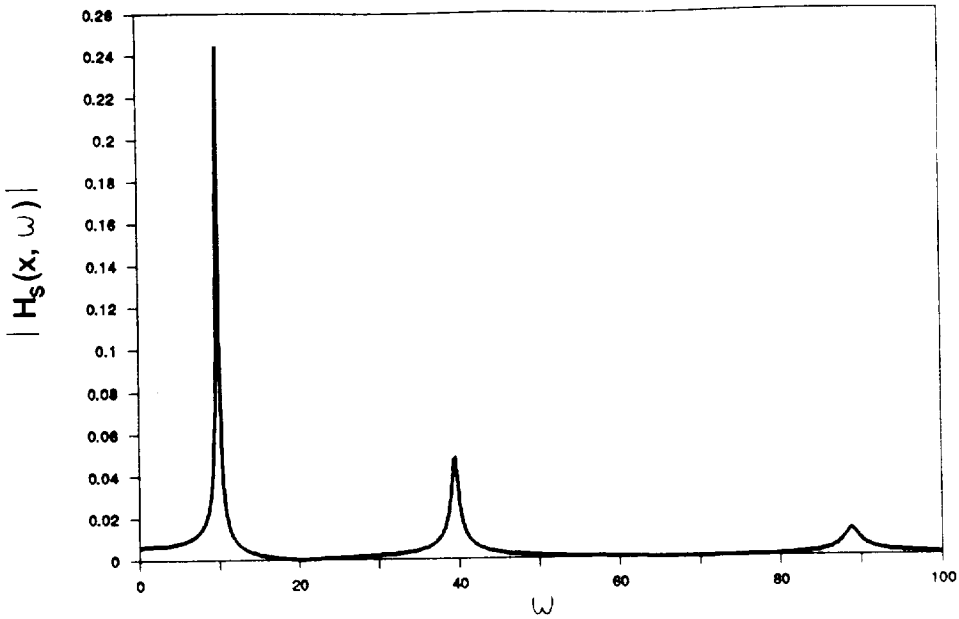

Figure 2a. Magnitude of the transfer function between exciting force and beam displacement at $x = 1/6$, $x_s = 1/6$, $\zeta_n = .01$

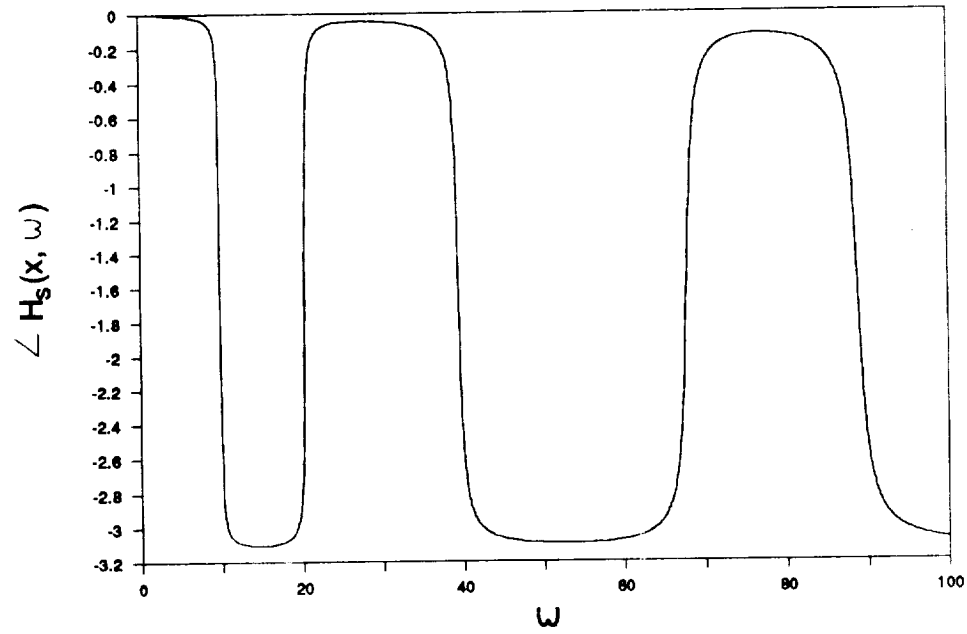

Figure 2b. Phase of the transfer function between exciting force and beam displacement at $x = 1/6$, $x_s = 1/6$, $\zeta_n = .01$

Chapter 3

CONTROLLING HARMONIC EXCITATION

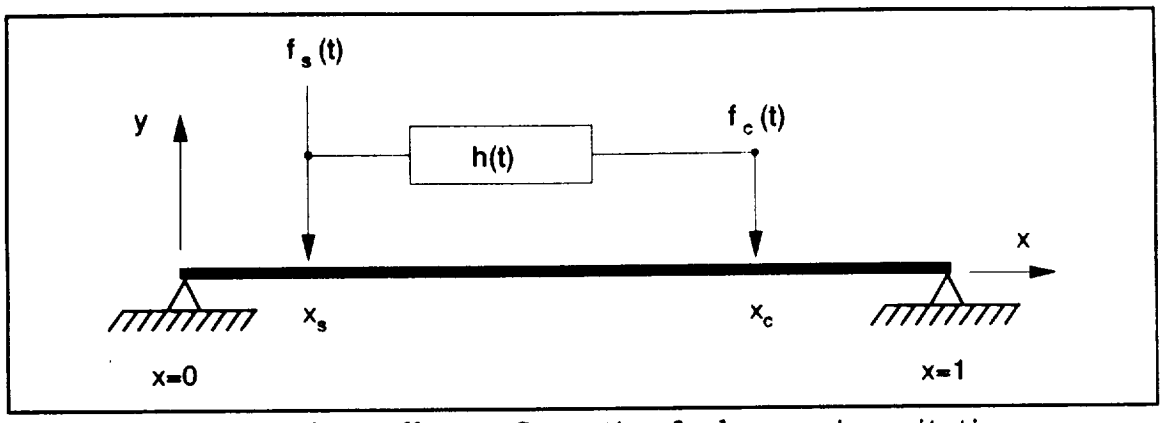

Figure 3. Controller configuration for harmonic excitation

In this chapter the force exciting the beam is assumed to be harmonic with an rms amplitude of unity. A second force is applied to control the steady-state vibrations of the beam. The arrangement of the exciting and controlling forces is shown in figure 3. The primary source of excitation is represented by $f_s(t)$ and the secondary force, used for controlling the beam, by $f_c(t)$. The linear relation between the exciting and controlling forces defines the controller. In the time domain this linear relation is written

$$f_c(t) = \int_{-\infty}^{\infty} d\tau\, h(\tau) f_s(t-\tau) \tag{24}$$

where $h(t)$ is the impulse response of the controller.

For harmonic excitation, the convolution in equation (24) becomes

$$\hat{f}_c = H(\omega)\hat{f}_s \tag{25}$$

where $H(\omega)$ is the Fourier transform[19] of the controller impulse response $h(t)$.

The displacement of the beam due to a harmonic point source was found in Chapter 2. Invoking superposition, the displacement due to both the exciting force and the controlling force is

$$\hat{y}(x,\omega) = H_s(x,\omega)\hat{f}_s + H_c(x,\omega)\hat{f}_c \tag{26}$$

where

$$H_s(x,\omega) = 2\sum_{n=1}^{\infty}\phi_n(x_s)\phi_n(x)H_n(\omega)$$

$$H_c(x,\omega) = 2\sum_{n=1}^{\infty}\phi_n(x_c)\phi_n(x)H_n(\omega) \tag{27}$$

and

$$H_n(\omega) = \frac{1}{\omega_n^2 - \omega^2 + 2j\omega\omega_n\zeta_n} \tag{28}$$

Using equation (25), equation (26) can be rewritten as

$$\hat{y}(x,\omega) = \{H_s(x,\omega) + H(\omega)H_c(x,\omega)\}\hat{f}_s \tag{29}$$

Combining equation (27) and (29) gives the harmonic equivalent of equation (6):

$$\hat{y}(x,\omega) = \sum_{n=1}^{\infty}\phi_n(x)\hat{y}_n(\omega) \tag{29.1}$$

where

$$\hat{y}_n(\omega) = \hat{f}_s\{\phi_n(x_s) + H(\omega)\phi_n(x_c)\}H_n(\omega) \tag{29.2}$$

Note that equation (29) reveals that a controller can be found such that the displacement is equal to zero at any single point x on the beam. This controller is given by

$$H(\omega) = -\frac{H_s(x,\omega)}{H_c(x,\omega)} \tag{30}$$

For harmonic excitation, the vibration of the beam will be represented by the mean square displacement. Integrating the mean square displacement over some length of the beam results in a cost function to be minimized. Define

$$\Phi \equiv \int_{x_1}^{x_2} dx\, \overline{y^2(x,t)} \tag{31}$$

where the bar denotes a time average. The controller that minimizes this functional is the controller that reduces the mean square displacement, integrated over the specified length of the beam, to the smallest value possible with the given beam configuration. This point is stressed because, in some cases, this may not be the quantity that is desired to be minimized, and if not, the appropriate quantity should be defined.

Since squaring is not a linear operation, the real part of the complex displacement must be taken before squaring:

$$y^2(x,t) = \Re^2\{|\, \hat{y}(x,\omega)\,|\, e^{j[\omega t + \theta(x,\omega)]}\} \tag{32}$$

where $\theta(x,\omega)$ is the phase angle of $\hat{y}(x,\omega)$. Now take the real part and square it to give

$$y^2(x,t) = |\, \hat{y}(x,\omega)\,|^2 \cos^2[\omega t + \theta(x,\omega)]$$

which can be split into a constant and an oscillating part by the trigonometric double angle formula, resulting in

$$y^2(x,t) = \frac{1}{2}|\, \hat{y}(x,\omega)\,|^2 \{1 + \cos[2\omega t + 2\theta(x,\omega)]\} \tag{34}$$

Taking the time average of equation (34) and substituting it into equation (31) gives

$$\Phi(\omega) = \frac{1}{2}\int_{x_1}^{x_2} dx\, |\, \hat{y}(x,\omega)\,|^2 \tag{35}$$

Equation (29) can now be substituted into equation (35), giving the functional to be minimized in terms of the sought controller function $H(\omega)$:

$$\Phi(\omega) = \int_{x_1}^{x_2} dx \mid H_s(x,\omega) + H(\omega)H_c(x,\omega) \mid^2 \frac{\mid \hat{f}_s \mid^2}{2} \tag{35.1}$$

Notice that $\mid \hat{f}_s \mid^2 /2$ is the rms amplitude of the sinusoidal excitation which has been assumed to be unity so equation (35.1) can be written

$$\Phi(\omega) = \int_{x_1}^{x_2} dx \mid H_s(x,\omega) + H(\omega)H_c(x,\omega) \mid^2 \tag{36}$$

Equation (36) can be expanded in the form

$$\Phi(\omega) = B_1(\omega) + B_2^*(\omega)H(\omega) + B_2(\omega)H^*(\omega) + B_3(\omega) \mid H(\omega) \mid^2 \tag{37}$$

where

$$B_1(\omega) \equiv \int_{x_1}^{x_2} dx \mid H_s(x,\omega) \mid^2$$

$$B_2(\omega) \equiv \int_{x_1}^{x_2} dx\, H_s(x,\omega)H_c^*(x,\omega)$$

$$B_3(\omega) \equiv \int_{x_1}^{x_2} dx \mid H_c(x,\omega) \mid^2 \tag{38}$$

Equation (37) cannot be minimized by taking the derivative with respect to $H(\omega)$ and setting it equal to zero because the derivative is not defined for complex conjugation. However, the derivative with respect to the real and imaginary parts of $H(\omega)$ is defined. Let

$$H(\omega) = R(\omega) + jI(\omega) \tag{39}$$

where $R(\omega)$ and $I(\omega)$ are the real and imaginary parts of $H(\omega)$ respectively. Substituting equation (39) into (37) results in

$$\Phi(\omega) = B_1(\omega) + B_2^*(\omega)\{R(\omega) + jI(\omega)\} + B_2(\omega)\{R(\omega) - jI(\omega)\} + B_3(\omega)\{R^2(\omega) + I^2(\omega)\} \tag{39.5}$$

Now take the partial derivative with respect to $R(\omega)$ and $I(\omega)$:

$$\frac{\partial \Phi}{\partial R} = B_2^* + B_2 + 2B_3 R(\omega)$$

$$\frac{\partial \Phi}{\partial I} = j(B_2^* - B_2) + 2B_3 I(\omega) \tag{40}$$

Set these derivatives equal to zero and solve for $R(\omega)$ and $I(\omega)$. Putting the results back into equation (39) yields the optimal controller:

$$H(\omega) = -\frac{B_2(\omega)}{B_3(\omega)} \tag{41}$$

Using this in equation (37) gives the minimum value of Φ:

$$\Phi(\omega) = B_1(\omega) - \frac{|B_2(\omega)|^2}{B_3(\omega)} \tag{41.1}$$

Now use equation (38) to rewrite (41):

$$H(\omega) = \frac{-\int_{x_1}^{x_2} dx\, H_s(x,\omega) H_c^*(x,\omega)}{\int_{x_1}^{x_2} dx\, |H_c(x,\omega)|^2} \tag{42}$$

It may provide some insight to look at some special cases of equation (42). It can be expanded over the modes by using equation (27):

$$H(\omega) = \frac{-\sum_{n=1}^{\infty}\sum_{m=1}^{\infty} H_n(\omega) H_m^*(\omega) \phi_n(x_s)\phi_m(x_c) \int_{x_1}^{x_2} dx\, \phi_n(x)\phi_m(x)}{\sum_{n=1}^{\infty}\sum_{m=1}^{\infty} H_n(\omega) H_m^*(\omega) \phi_n(x_c)\phi_m(x_c) \int_{x_1}^{x_2} dx\, \phi_n(x)\phi_m(x)} \tag{43}$$

If Φ is to be minimized over the length of the beam, $x_1 = 0$ and $x_2 = 1$. Because the eigenfunctions are orthogonal over this interval, equation (43) reduces to

$$H(\omega) = \frac{-\sum_{n=1}^{\infty} |H_n(\omega)|^2 \phi_n(x_s)\phi_n(x_c)}{\sum_{n=1}^{\infty} |H_n(\omega)|^2 \phi_n^2(x_c)} \tag{43.1}$$

The frequency response of the controller in equation (43.1) is real, which implies that the impulse response of the controller is even[19]. This can be seen by writing the inverse Fourier transform

$$h(t) = \frac{1}{2\pi}\int_{-\infty}^{\infty} d\omega H(\omega) e^{j\omega t} \tag{43.2}$$

and its complex conjugate,

$$h(t) = \frac{1}{2\pi}\int_{-\infty}^{\infty} d\omega H^{*}(\omega) e^{-j\omega t} \tag{43.3}$$

Since by equation (43.1), $H(\omega) = H^{*}(\omega)$, it can now be seen from equation (43.3) that $h(t) = h(-t)$. The impact of the even impulse function can be seen by looking back to equation (24). To find the controlling force $f_c(t)$, *future* values of the excitation force $f_s(t)$ are required since $h(-t) \neq 0$. For this reason the controller is referred to as acausal. If the future values of the excitation cannot be predicted, an acausal controller cannot be used in a real-time application. Obviously the future is predictable for harmonic excitation and causality is not a constraint[20].

Now that the controller that minimizes Φ over the entire length of the beam has been found, it is interesting to compare it with the controller that minimizes Φ at a single point. This controller can be found by letting the interval of minimization approach zero, i.e. $|x_2 - x_1| \rightarrow 0$ where the point of interest is between x_1 and x_2. In the limit, the integrands in equation (42) can be treated as constant and taken outside of the integrations. This results in

$$H(\omega) = \frac{-H_s(x,\omega)H_c^{*}(x,\omega)}{|H_c(x,\omega)|^2} \tag{44}$$

which simplifies to

$$H(\omega) = -\frac{H_s(x,\omega)}{H_c(x,\omega)} \tag{45}$$

Equation (45) gives the optimal controller for minimizing the mean square displacement at a single point on the beam. This agrees with the result of equation (30) and from equation (29) it can be seen that the mean square displacement at this point is zero.

Another configuration that can be evaluated analytically is that for which the exciting and controlling force are collocated, i.e. $x_s = x_c \Rightarrow H_s(x,\omega) = H_c(x,\omega)$. It can be seen from equation (42) that $H(\omega) = -1$ which implies that $h(t) = -\delta(t)$. Using the definition of $h(t)$ given in equation (24),

$$f_c(t) = -\int_{-\infty}^{\infty} d\tau\, \delta(\tau) f_s(t-\tau) = -f_s(t) \tag{46}$$

which results in perfect control as expected when substituted back into equation (36).

The best controller for harmonic excitation has been found and the limiting cases of control checked. Now a digital computer will be used to obtain limits on control for more general arrangements. Calculating the amplitude of $\hat{y}(x,\omega)$ in equation (29.1) gives the envelope of the beam displacement. This amplitude is plotted versus the non-dimensional length x of the beam, before and after control, for several excitation frequencies in figures 4-7. A table of modal coefficients accompanies each figure. The tables reveal the effect of the controller on the magnitude and phase of the individual modes. Although all results are presented without dimension, it is

necessary to state that the phase will be expressed in radians throughout this thesis. Only the first three modes are considered and the coefficient of damping ζ_n for all modes is taken to be 1%.

In both figures 4 and 5, the driving frequency is at resonance of the second mode. In figure 4, Φ is being minimized globally or over the entire length of the beam, $0 \le x \le 1$, while in figure 5, it is being minimized locally or over a subinterval, $3/4 \le x \le 1$. Because the displacement of the beam is dominated by the response of a single mode, minimizing the cost function Φ locally results in very nearly the same global performance as when minimizing globally.

The contributions of the individual modes when minimizing globally are given in table 1. Before control, the second mode clearly dominates the displacement. Notice the phase of the individual modes before control. These are given relative to the exciting source. The third mode has a phase lag of ≈ 0 because it is being excited below resonance; the second mode has a phase lag of $\approx \pi/2$ because it is excited near resonance; the first mode has a phase lag of $\approx \pi$ because it is excited above resonance. After control, the phases are unchanged. The reason for this can be revealed by examination of equation (29.2). When minimizing Φ over the length of the beam, $H(\omega)$ is real (see eqn. 43.1), so it cannot affect the phase of the nth modal coefficient, $\hat{y}_n(\omega)$. Assuming a reference phase of zero for the excitation source, the phase of the nth modal coefficient is

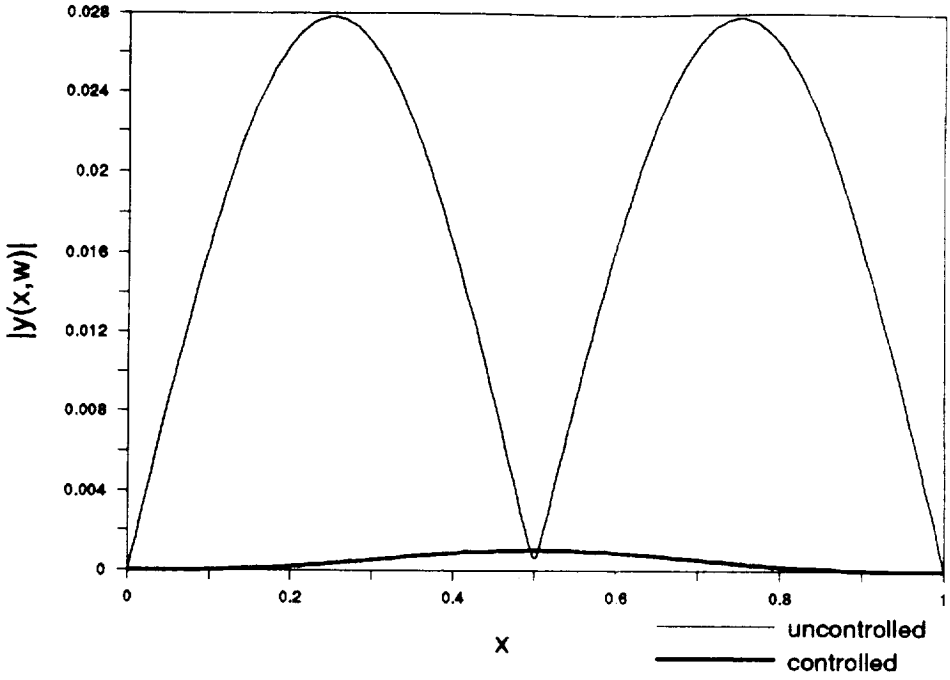

Figure 4. Envelope of beam displacement, $x_s = 1/6$, $x_c = 3/4$, $x_1 = 0$, $x_2 = 1$, $\omega = \omega_2$

	Before Control		After Control	
Mode n	$\lvert \hat{y}_n(\omega) \rvert$	$\angle \hat{y}_n(\omega)$	$\lvert \hat{y}_n(\omega) \rvert$	$\angle \hat{y}_n(\omega)$
1	4.839E-04	-3.136E+00	1.076E-03	-3.136E+00
2	3.929E-02	-1.571E+00	1.749E-05	-1.571E+00
3	2.233E-04	-1.107E-02	3.600E-04	-1.107E-02

Table 1. Modal coefficients before and after control for figure 4.

$$\angle \hat{y}_n(\omega) = \angle H_n(\omega) = -\tan^{-1}\left\{\frac{2\omega\omega_n\zeta_n}{\omega_n^2 - \omega^2}\right\} \tag{46.1}$$

The modal phases are fixed before a controller is ever found! This explains why the phases are unchanged after control in table 1. The amplitude of the second mode, which is at resonance, is greatly reduced. When minimizing locally in figure 5, the amplitude of the second mode was not as dramatically

reduced. This allowed slightly better control within the control interval. When the beam was excited at resonant frequencies of the other modes, the beam displayed very similar behavior as that seen in figures 4 and 5.

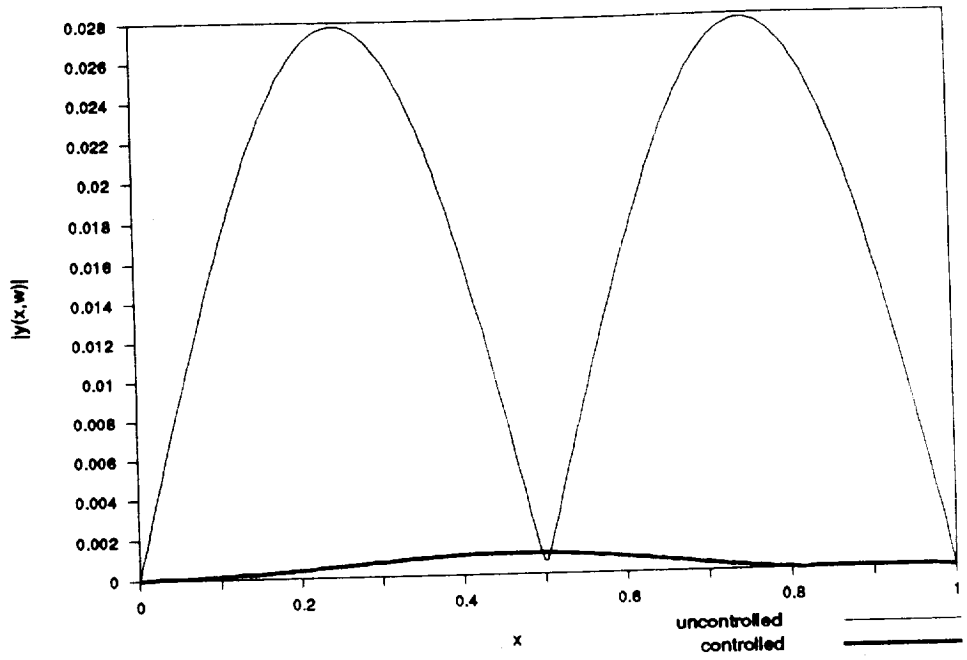

Figure 5. Envelope of beam displacement, $x_s = 1/6$, $x_c = 3/4$, $x_1 = 3/4$, $x_2 = 1$, $\omega = \omega_2$

	Before Control		After Control	
Mode n	$\lvert \hat{y}_n(\omega) \rvert$	$\angle \hat{y}_n(\omega)$	$\lvert \hat{y}_n(\omega) \rvert$	$\angle \hat{y}_n(\omega)$
1	4.839E-04	-3.136E+00	1.076E-03	-3.132E+00
2	3.929E-02	-1.571E+00	2.572E-04	-3.105E+00
3	2.233E-04	-1.107E-02	3.600E-04	-8.591E-03

Table 2. Modal coefficients before and after control for figure 5.

Figures 6 and 7 are the same as figures 4 and 5 described above except for the driving frequency. For these cases, the driving frequency is between the first and second natural frequencies of the beam. Minimizing Φ over the

length of the beam in figure 6 shows virtually no control at all. To understand why this is so, use equation (29.1) to expand equation (35) over the modes, resulting in

$$\Phi(\omega) = \frac{1}{2} \sum_{n=1}^{\infty} \sum_{m=1}^{\infty} \hat{y}_n(\omega) \hat{y}_m^*(\omega) \int_{x_1}^{x_2} dx\, \phi_n(x) \phi_m(x) \tag{46.2}$$

which simplifies to

$$\Phi(\omega) = \frac{1}{4} \sum_{n=1}^{\infty} | \hat{y}_n(\omega) |^2 \tag{46.3}$$

when calculating Φ over the beam length. This equation reveals that the modal amplitudes $| \hat{y}_n(\omega) |$ must be independently controlled for global reduction of Φ. The table of modal coefficients for figure 6 implies that excellent control can be obtained if the coefficients of the first and second modal amplitudes can be independently reduced, but this is not possible because the controller $H(\omega)$ has only one degree of freedom when minimizing Φ globally (see eqn. 43.1).

Between resonances, two modes are contributing on the same order to the total response of the beam. Therefore, controlling one mode excites the other even more, and this spillover limits the amount of control that is possible when minimizing globally. When minimizing locally, the controller uses spillover to achieve better control as seen in figure 7. Notice that the beam displacement outside the subinterval of control is much larger than before the control was applied. Table 4 gives the contributions of the individual modes to the displacement envelope in figure 7. The amplitudes of all three modes are increased significantly, but the phase of the second mode was changed so as to cancel the contributions of the first and third mode in the interval of minimization which created a larger displacement envelope

outside the interval of minimization. It will be seen in figure 14 that moving the location of the controller allows better control both inside and outside of the minimization interval.

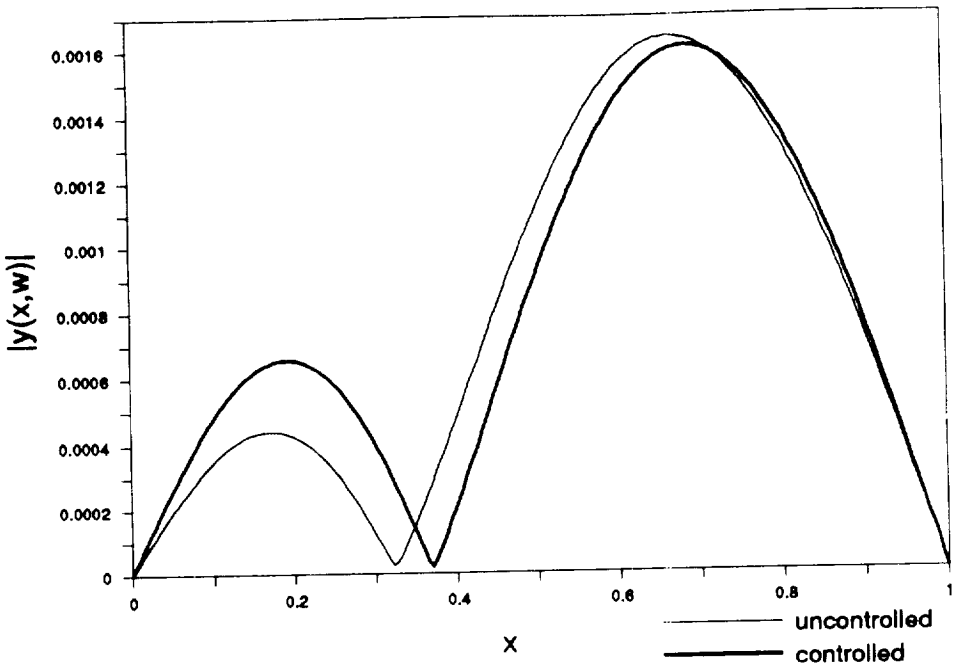

Figure 6. Envelope of beam displacement, $x_s = 1/6$, $x_c = 3/4$, $x_1 = 0$, $x_2 = 1$, $\omega = 2.5\omega_1$

	Before Control		After Control	
Mode n	$\lvert \hat{y}_n(\omega) \rvert$	$\angle \hat{y}_n(\omega)$	$\lvert \hat{y}_n(\omega) \rvert$	$\angle \hat{y}_n(\omega)$
1	1.382E-03	-3.132E+00	1.120E-03	-3.132E+00
2	1.289E-03	-2.050E-02	1.488E-03	-2.050E-02
3	1.942E-04	-6.019E-03	1.758E-04	-6.019E-03

Table 3. Modal coefficients before and after control for figure 6.

Now that the beam displacement envelope has been examined for several cases and the amount of reduction over the length of the beam seen, it is interesting to study the reduction of Φ, which corresponds to the

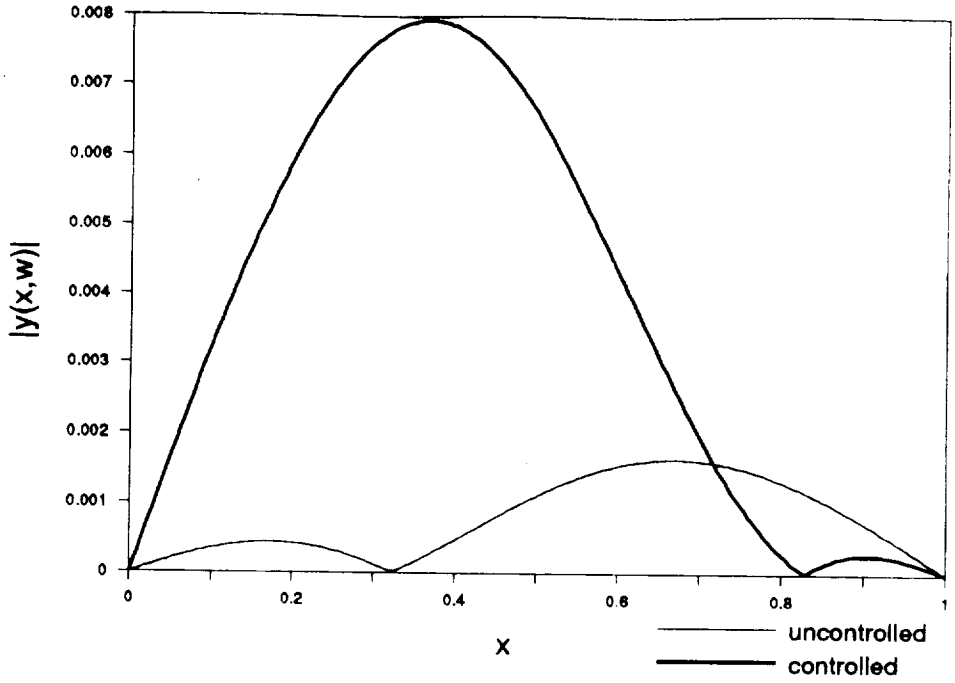

Figure 7. Envelope of beam displacement, $x_s = 1/6$, $x_c = 3/4$, $x_1 = 3/4$, $x_2 = 1$, $\omega = 2.5\omega_1$

	Before Control		After Control	
Mode n	$\lvert \hat{y}_n(\omega) \rvert$	$\angle \hat{y}_n(\omega)$	$\lvert \hat{y}_n(\omega) \rvert$	$\angle \hat{y}_n(\omega)$
1	1.382E-03	-3.132E+00	8.614E-03	-3.061E+00
2	1.289E-03	-2.050E-02	4.226E-03	-3.052E+00
3	1.942E-04	-6.019E-03	7.019E-04	5.494E-02

Table 4. Modal coefficients before and after control for figure 7.

performance of the controller. Without control, it can be seen from equation (37) that $\Phi = B_1(\omega)$. After applying control, Φ is given by equation (41.1). These two quantities are compared in figures 8-13.

Figures 8 and 9 give the performance of the controller versus frequency for minimizing over the beam length, and over a subinterval of the beam length, respectively. Figures 4-7 become single data points on these graphs. The largest reduction of Φ is at the resonance frequencies in both figure 8 and

9. Notice that there is a frequency between the modes at which no control is possible. The exact frequency at which this occurs is a function of x_s and x_c. At this frequency there is a balance of the modal responses in the region of control, so spillover prevents any reduction of the cost function. The location of Figure 9 shows that a greater reduction in Φ is possible when minimizing over a subinterval of the beam length.

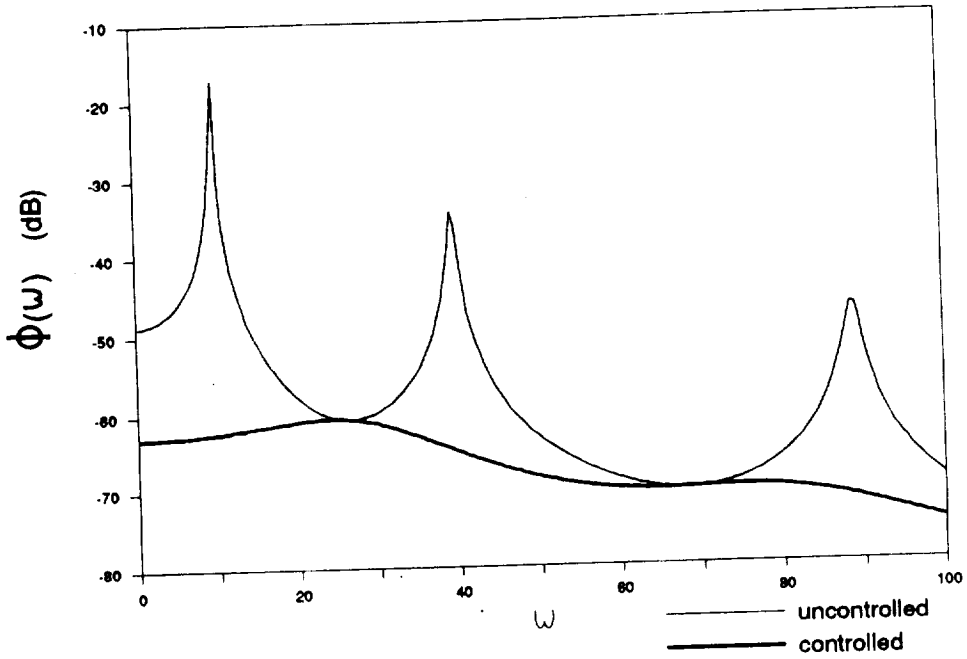

Figure 8. Effect of frequency on reduction of global cost function Φ, $x_s = 1/6$, $x_c = 3/4$, $x_1 = 0$, $x_2 = 1$

Figures 10-13 illustrate the importance of location of the controller if that freedom is available. All of these plots show the perfect control when the controller is collocated with the source. The beam is being driven at the resonant frequency of the second mode in figures 10 and 11. Note that insignificant global control is possible in figure 10 when the controller is located at a node of the mode that is dominating the displacement, but figure 11 shows that local control is always possible at a resonance, no matter

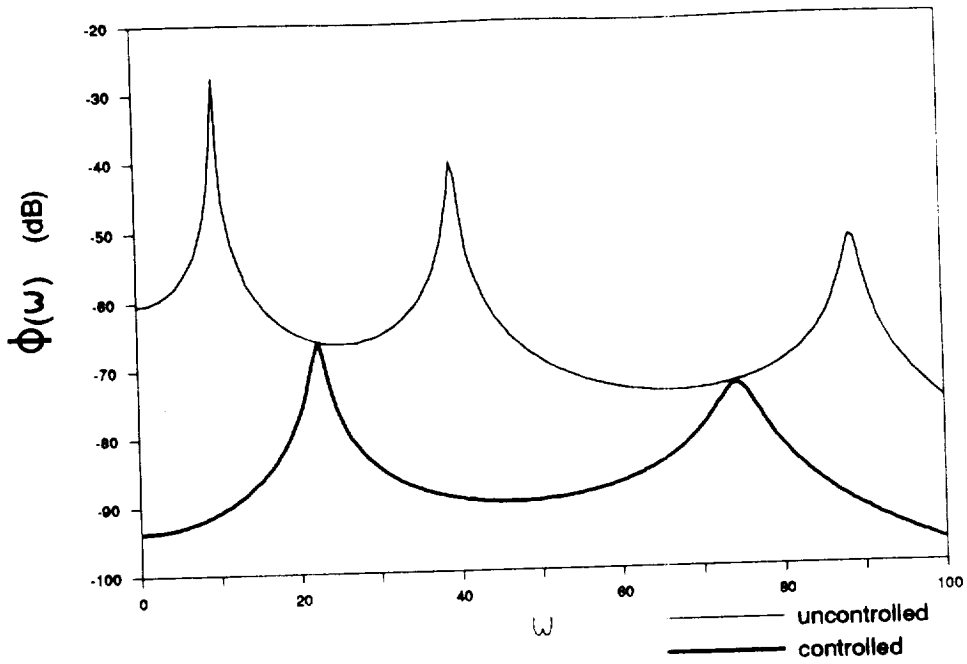

Figure 9. Effect of frequency on reduction of local cost function Φ, $x_s = 1/6$, $x_c = 3/4$, $x_1 = 3/4$, $x_2 = 1$

where the controller is located.

In figures 12 and 13 the driving frequency is between the first and second natural frequencies. If one is trying to control globally, figure 12 shows that it is best to be as close as possible to the source. When minimizing locally, a more complex relationship results, as shown in figure 13. Interestingly enough, the best control is achieved (for separated sources), when the controller is located at the center. At this position the controller cannot excite the second mode and as a result avoids spillover which allows greater freedom in altering the first and third modes, and results in much better control. This is the location of the controller in figure 14, in which all parameters are identical to those in figure 7, except for the controller location. It can be noted from table 5 that the second mode is not excited by the controller, because the amplitude and phase are unchanged after control.

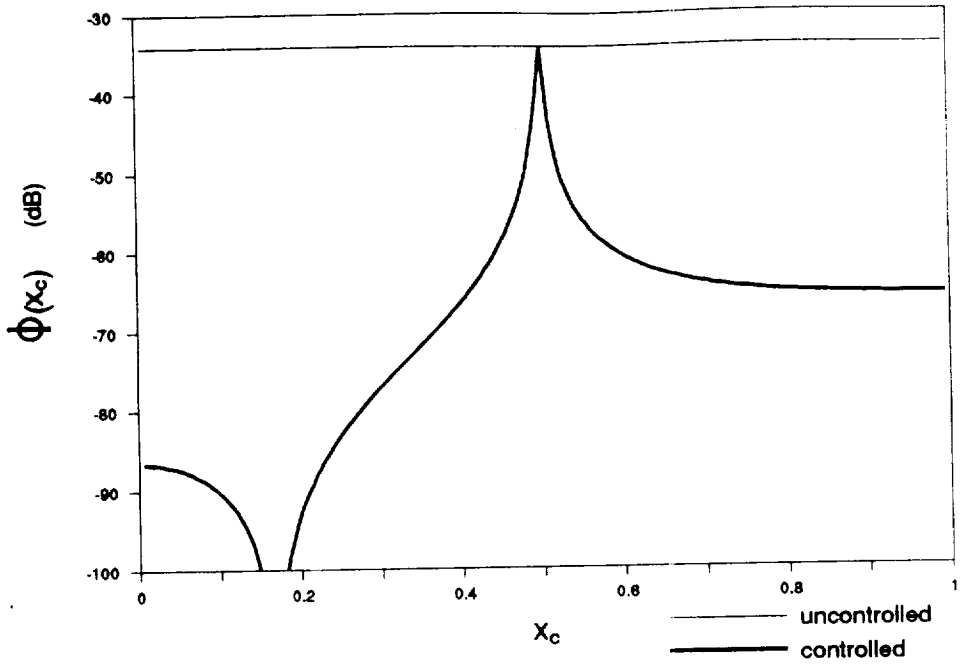

Figure 10. Effect of controller position x_c on reduction of global cost function Φ, $x_s = 1/6$, $x_1 = 0$, $x_2 = 1$, $\omega = \omega_2$

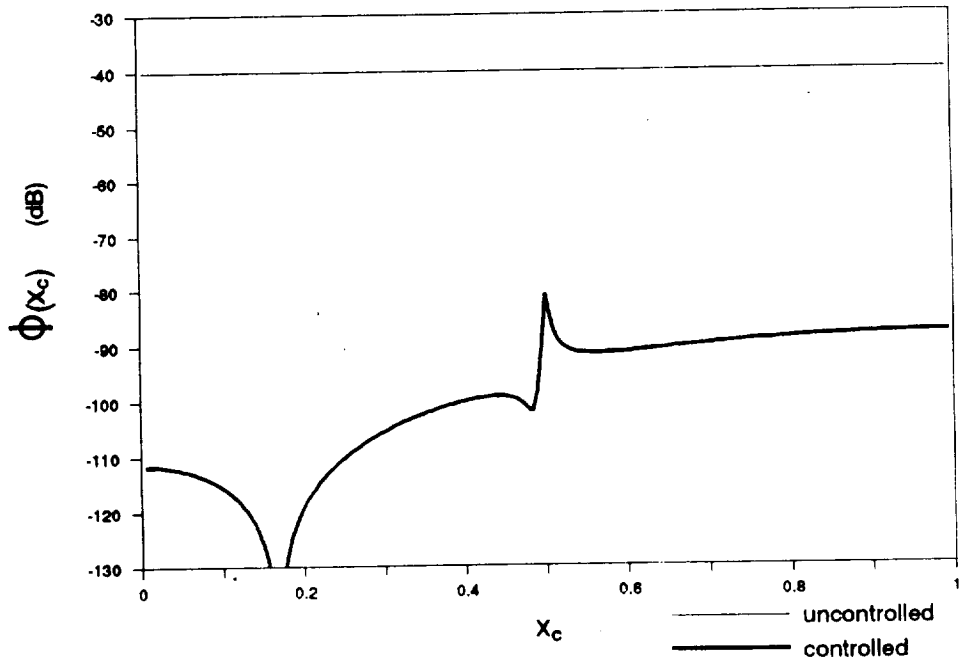

Figure 11. Effect of controller position x_c on reduction of local cost function Φ, $x_s = 1/6$, $x_1 = 3/4$, $x_2 = 1$, $\omega = \omega_2$

The amplitudes of the first and third modes are increased and the phase of the first mode is shifted by π, so that the optimal control is achieved by a destructive interference between the modes in the region of minimization.

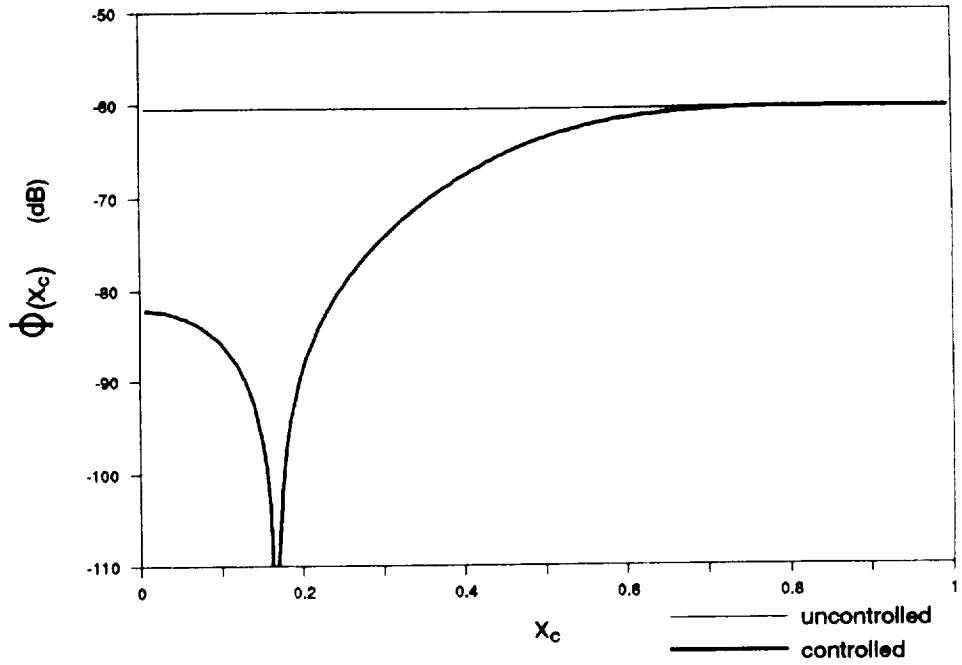

Figure 12. Effect of controller position x_c on reduction of global cost function Φ, $x_s = 1/6$, $x_1 = 0$, $x_2 = 1$, $\omega = 2.5\omega_1$

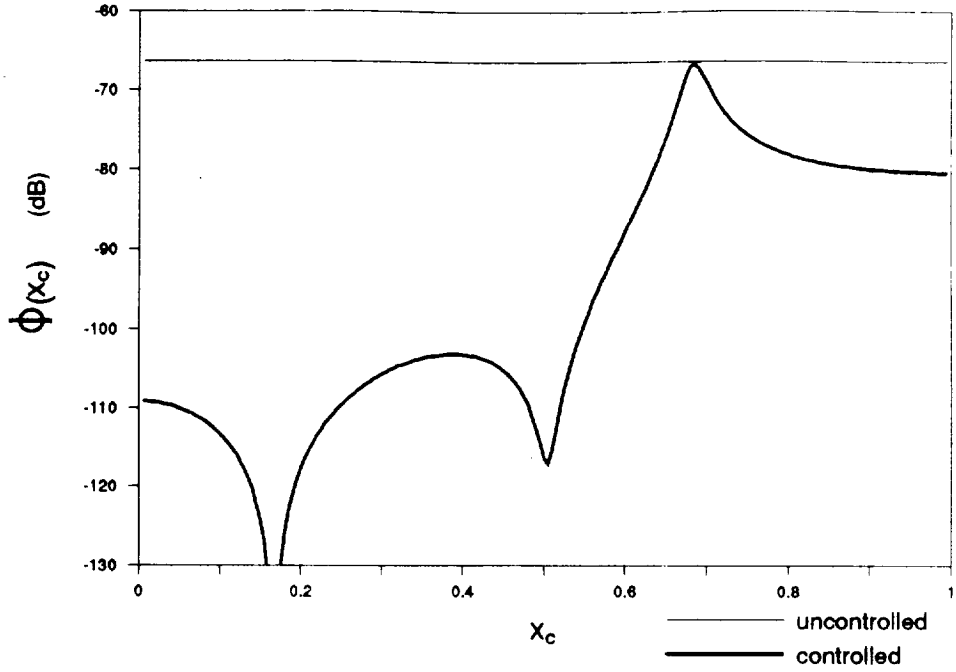

Figure 13. Effect of controller position x_c on reduction of local cost function Φ, $x_s = 1/6$, $x_1 = 3/4$, $x_2 = 1$, $\omega = 2.5\omega_1$

Figures 7 and 14 illustrate control of the beam over an interval. In figure 7 control was possible at the cost of a considerable increase in displacement outside of the interval of minimization. In figure 14, much better control was shown to be possible with smaller displacements outside the interval of minimization with the proper location of the controller. For these same two locations of the controller, it is interesting to examine the effect of a continuous change in the interval of minimization. Comparing the global cost function to that obtained when minimizing locally (over a subinterval), gives an indication of the efficiency of the controller. To do this, fix the right side of the interval at $x_2 = 1$ and let $0 < x_1 < 1$. The ideal controller is then found from equation (41) and Φ from equation (37).

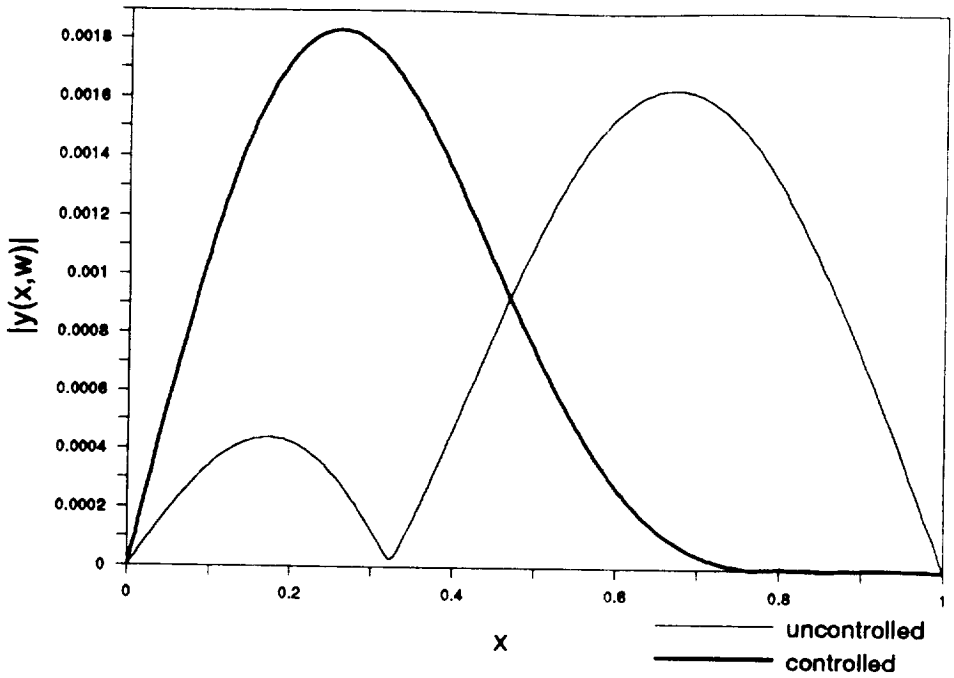

Figure 14. Envelope of beam displacement before and after local minimization with optimal controller placement, $x_s = 1/6$, $x_c = 1/2$, $x_1 = 3/4$, $x_2 = 1$, $\omega = 2.5\omega_1$

	Before Control		After Control	
Mode n	$\lvert \hat{y}_n(\omega) \rvert$	$\angle \hat{y}_n(\omega)$	$\lvert \hat{y}_n(\omega) \rvert$	$\angle \hat{y}_n(\omega)$
1	1.382E-03	-3.132E+00	1.441E-03	-2.339E-02
2	1.289E-03	-2.050E-02	1.289E-03	-2.050E-02
3	1.942E-04	-6.019E-03	3.925E-04	-1.451E-02

Table 5. Modal coefficients before and after control for figure 14.

Figure 15 shows almost no increase in the global cost function when the interval of minimization is changed. This indicates that minimizing locally is the same as minimizing globally. When any single mode dominates the total response of the beam, then minimizing the response of that mode results in both a global and local minimum. The result is much different if the exciting source is off resonance, as can be seen in figure 16. In this case, the global cost function Φ increases dramatically to allow greater minimization in the

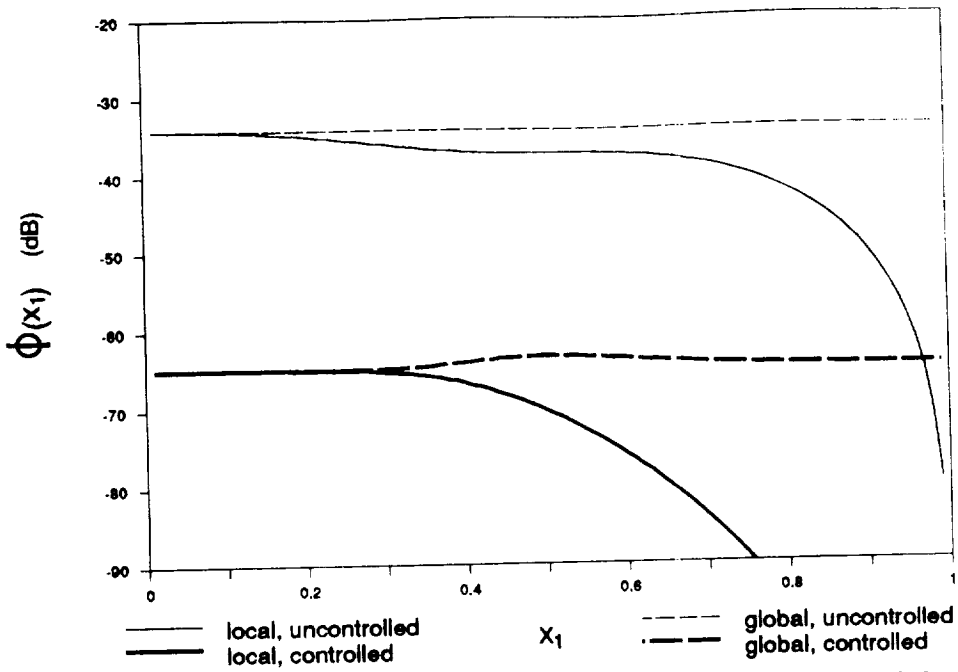

Figure 15. Effect of interval of minimization on both the global and local value of cost function Φ before and after control, $\omega = \omega_2$, $x_s = 1/6$, $x_c = 3/4$, $x_2 = 1$

interval of concern. This is a result of spillover being utilized to reduce Φ locally. If the controller is located optimally, this increase in the global cost function Φ, due to spillover, can be minimized as shown in figure 17. It can be seen that with the proper location of the controller, tremendous reduction in Φ can be achieved locally without a significant increase in the global value of Φ.

In summary, the best control of harmonic excitation over the length of the beam is achieved when the displacement is dominated by one mode. Over the length of the beam, the modes must be independently minimized and a single controller can only independently minimize a single mode. If control is desired only over a subregion, it is possible to control all modes over this subregion if spillover outside of the region of control is allowed. In general, the best location for the controller is as close as possible to the exciting

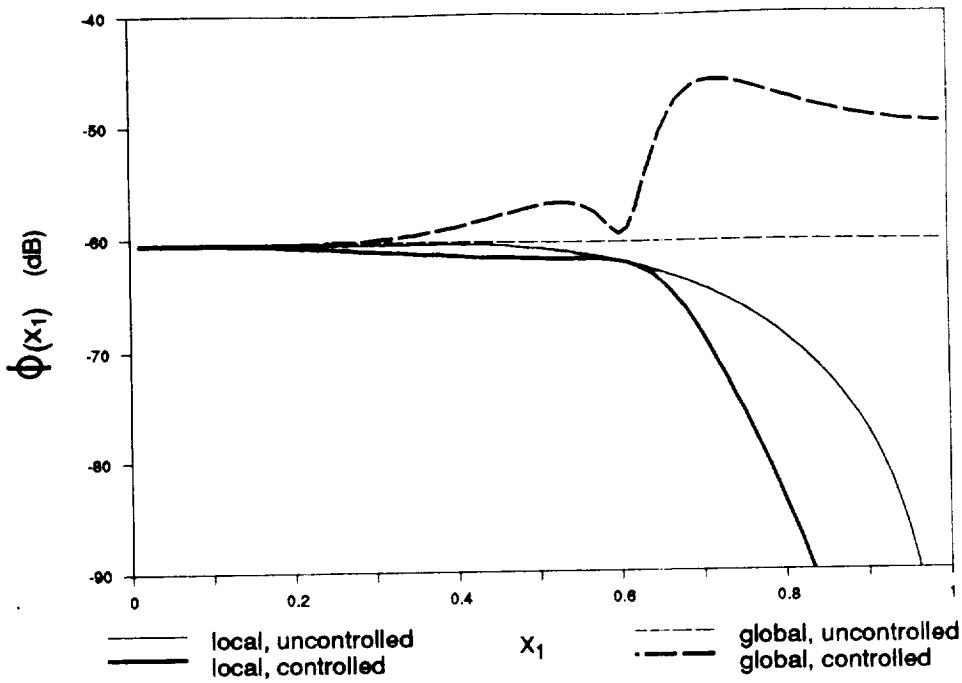

Figure 16. Effect of interval of minimization on both the global and local value of cost function Φ before and after control, $\omega = 2.5\omega_1$, $x_s = 1/6$, $x_c = 3/4$, $x_2 = 1$

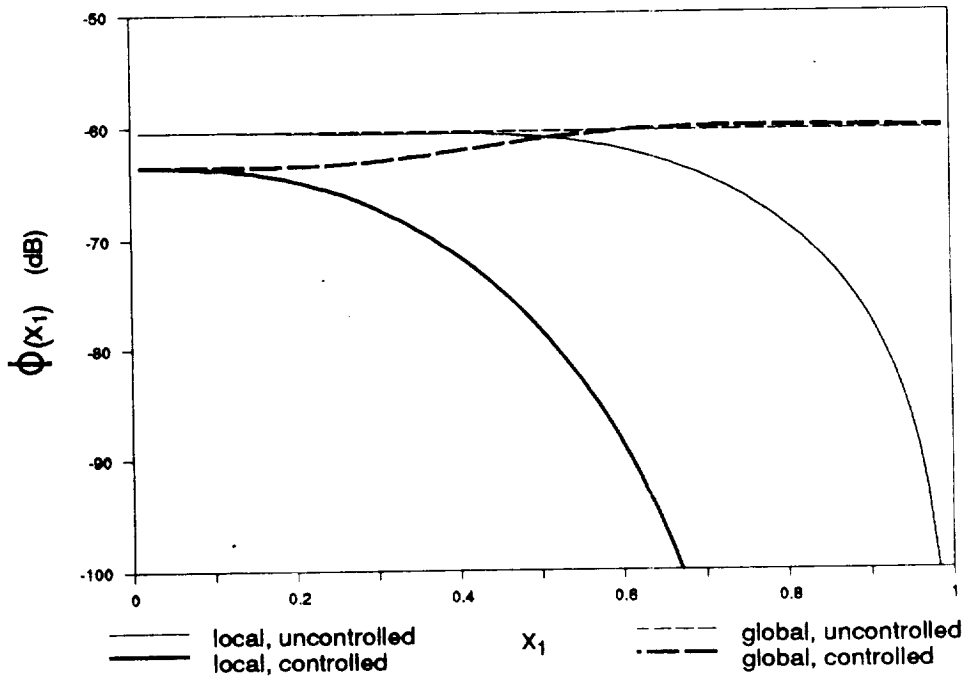

Figure 17. Effect of interval of minimization on both the global and local value of cost function Φ before and after control with x_c optimal, $\omega = 2.5\omega_1$, $x_s = 1/6$, $x_c = 1/2$, $x_2 = 1$

source. Results similar to these presented have been seen in experimental control of a semi-infinite beam[9], which would seem to indicate that comparable mechanisms are present for other types of boundary conditions.

Chapter 4

CONTROLLING RANDOM EXCITATION

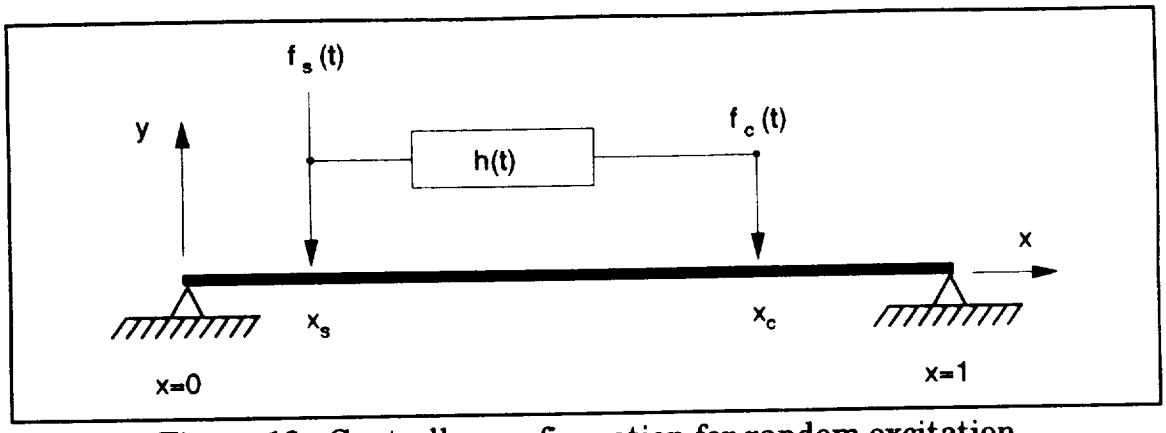

Figure 18. Controller configuration for random excitation

In this chapter the force exciting the beam is assumed to be a random process with a constant power spectrum and a variance of unity. This type of random process is also referred to as white noise because of its uniform frequency content. A second force is applied to control the stationary vibrations of the beam. The arrangement of the exciting and controlling forces is shown in figure 18. The primary source of excitation is represented by $f_s(t)$ and the secondary force, used for controlling the beam, by $f_c(t)$. The linear relation between the exciting and controlling forces defines the controller. In the time domain this linear relation is written

$$f_c(t) = \int_{-\infty}^{\infty} d\tau\, h(\tau) f_s(t-\tau) \tag{47}$$

where $h(t)$ is the impulse response of the controller.

The displacement of the beam due to a single exciting force is given by equation (17). By superposition, the total displacement is

$$y(x,t) = \int_0^\infty d\tau_1 h_s(x,\tau_1) f_s(t-\tau_1) + \int_0^\infty d\tau_1 h_c(x,\tau_1) f_c(t-\tau_1) \tag{48}$$

Using equation (47), this can be written

$$y(x,t) = \int_0^\infty d\tau_1 h_s(x,\tau_1) f_s(t-\tau_1) + \int_0^\infty d\tau_1 h_c(x,\tau_1) \int_{-\infty}^\infty d\tau h(\tau) f_s(t-\tau_1-\tau) \tag{49}$$

For random excitation the vibration of the beam will be represented by the expected value of the displacement squared. Integrating this quantity over some length of the beam results in a cost functional to be minimized with respect to the impulse response function of the controller. Define

$$\Psi \equiv \int_{x_1}^{x_2} dx\, \sigma_y^2(x) \tag{50}$$

as this cost functional where, $\sigma_y^2(x)$ is the variance of the displacement which is identical to the expected value of the displacement squared. To find Ψ in terms of $h(t)$, the impulse response of the controller, first square equation (49)

$$\begin{aligned} y^2(x,t) = & \int_0^\infty d\tau_1 d\tau_2 h_s(x,\tau_1) h_s(x,\tau_2) f_s(t-\tau_1) f_s(t-\tau_2) \\ & + 2\int_{-\infty}^\infty d\tau h(\tau) \int_0^\infty d\tau_1 d\tau_2 h_s(x,\tau_1) h_c(x,\tau_2) f_s(t-\tau_1) f_s(t-\tau_2-\tau) \\ & + \int_{-\infty}^\infty d\tau d\tau' h(\tau) h(\tau') \int_0^\infty d\tau_1 d\tau_2 h_c(x,\tau_1) h_c(x,\tau_2) f_s(t-\tau_1-\tau) f_s(t-\tau_2-\tau') \end{aligned} \tag{51}$$

and then calculate the expected value,

$$\sigma_y^2(x) = \int_0^\infty d\tau_1 d\tau_2 R_{f_s}(\tau_1 - \tau_2) h_s(x,\tau_1) h_s(x,\tau_2)$$

$$+2\int_{-\infty}^{\infty} d\tau h(\tau) \int_0^\infty d\tau_1 d\tau_2 R_{f_s}(\tau_1 - \tau_2 - \tau) h_s(x,\tau_1) h_c(x,\tau_2)$$

$$+\int_{-\infty}^{\infty} d\tau d\tau' h(\tau) h(\tau') \int_0^\infty d\tau_1 d\tau_2 R_{f_s}(\tau_1 - \tau_2 + \tau - \tau') h_c(x,\tau_1) h_c(x,\tau_2) \qquad (51.1)$$

where $R_{f_s}(\tau)$ is the autocorrelation of the random process $f_s(t)$. For white noise with unity variance, $R_{f_s}(\tau) = \delta(\tau)$. Using this in equation (51.1) and integrating with respect to τ_2 yields

$$\sigma_y^2(x) = \int_0^\infty d\tau_1 h_s^2(x,\tau_1)$$

$$+2\int_{-\infty}^{\infty} d\tau h(\tau) \int_0^\infty d\tau_1 h_s(x,\tau_1) h_c(x,\tau_1 - \tau)$$

$$+\int_{-\infty}^{\infty} d\tau d\tau' h(\tau) h(\tau') \int_0^\infty d\tau_1 h_c(x,\tau_1) h_c(x,\tau_1 + \tau - \tau') \qquad (51.2)$$

The cost functional Ψ is found by integrating equation (51.2) over some length of the beam:

$$\Psi = b_1(0) + 2\int_{-\infty}^{\infty} d\tau h(\tau) b_2(\tau) + \int_{-\infty}^{\infty} d\tau d\tau' h(\tau) b_3(\tau - \tau') h(\tau') \qquad (53)$$

where

$$b_1(\tau) \equiv \int_0^\infty d\tau_1 \int_{x_1}^{x_2} dx\, h_s(x,\tau_1) h_s(x,\tau_1 - \tau)$$

$$b_2(\tau) \equiv \int_0^\infty d\tau_1 \int_{x_1}^{x_2} dx\, h_s(x,\tau_1) h_c(x,\tau_1 - \tau)$$

$$b_3(\tau) \equiv \int_0^\infty d\tau_1 \int_{x_1}^{x_2} dx\, h_c(x,\tau_1) h_c(x,\tau_1 - \tau) \qquad (54)$$

The Fourier transform of $b_1(\tau)$, $b_2(\tau)$, and $b_3(\tau)$ in equation (54) results in $B_1(\omega)$, $B_2(\omega)$, and $B_3(\omega)$, respectively. These transforms have previously been determined in equation (40). Now use the definition of the inverse Fourier transform defined by equation (21.2) to find Ψ in the frequency domain:

$$\Psi = \frac{1}{2\pi}\int_{-\infty}^{\infty} d\omega B_1(\omega)$$
$$+2\int_{-\infty}^{\infty} d\tau \frac{1}{4\pi^2}\int_{-\infty}^{\infty} d\omega_1 d\omega_2 H(\omega_1)B_2(\omega_2)e^{j(\omega_1+\omega_2)\tau}$$
$$+\int_{-\infty}^{\infty} d\tau d\tau' \frac{1}{8\pi^3}\int_{-\infty}^{\infty} d\omega_1 d\omega_2 d\omega_3 H(\omega_1)B_3(\omega_2)H(\omega_3)e^{j(\omega_1+\omega_2)\tau}e^{j(\omega_3-\omega_2)\tau'} \tag{55}$$

Using the identity[19]

$$\delta(\omega) = \frac{1}{2\pi}\int_{-\infty}^{\infty} d\tau e^{j\omega\tau} \tag{55.1}$$

equation (55) can be rewritten as

$$\Psi = \frac{1}{2\pi}\int_{-\infty}^{\infty} d\omega \{B_1(\omega) + 2B_2^*(\omega)H(\omega) + B_3(\omega)\,|\,H(\omega)\,|^2\} \tag{55.2}$$

From equation (53), notice that $B_2^*(\omega)H(\omega)$ must be a real quantity, so equation (55.2) can be rewritten as

$$\Psi = \frac{1}{2\pi}\int_{-\infty}^{\infty} d\omega \{B_1(\omega) + B_2^*(\omega)H(\omega) + B_2(\omega)H^*(\omega) + B_3(\omega)\,|\,H(\omega)\,|^2\} \tag{56}$$

From equation (37) it can be seen that the integrand of equation (56) is $\Phi(\omega)$, so it can be written

$$\Psi = \frac{1}{2\pi}\int_{-\infty}^{\infty} d\omega\, \Phi(\omega) \tag{57}$$

It is apparent from equation (36) that $\Phi(\omega)$ is an even function, so equation (57) can be written

$$\Psi = \frac{1}{\pi}\int_0^{\infty} d\omega\, \Phi(\omega) \tag{58}$$

With equation (36), equation (58) can be expanded into

$$\Psi = \int_{x_1}^{x_2} dx \frac{1}{\pi}\int_0^{\infty} d\omega |\, H_s(x,\omega) + H(\omega)H_c(x,\omega)\,|^2 \tag{59}$$

which, when compared to equation (50), gives

$$\sigma_y^2(x) = \frac{1}{\pi}\int_0^{\infty} d\omega |\, H_s(x,\omega) + H(\omega)H_c(x,\omega)\,|^2 \tag{60}$$

To minimize Ψ in equation (58), $\Phi(\omega)$ must be independently minimized at each value of ω, because the function $\Phi(\omega)$ is, by definition, positive for all ω. This independent minimization has already been accomplished in chapter 3. The unconstrained controller that gives the minimum vibration for harmonic excitation is also the best unconstrained controller for random excitation! After some thought, this fact is not so surprising. Without the constraint of causality, the impulse response of the controller is defined for $-\infty \le t \le \infty$. This has the effect of letting the controller "know" the input excitation before it excites the beam. Thus the random input is not random as seen by the controller, but deterministic. The infinite limits in equation (47) illustrate this mathematically. In this light, it makes sense that the optimum controller is the same for both random and periodic excitation.

Now that the unconstrained controller for random excitation is known, the performance of the controller will be examined. It is interesting to note that the special cases outlined in chapter 3 also hold for the case of random excitation; perfect control is achieved when the exciting source and controller

are collocated, and when minimizing the response at a single point on the beam. Because these cases result in $\Phi(\omega) \equiv 0$ for all values of ω, equation (58) verifies that the same holds for controlling random excitation.

For more general cases, the square root of equation (60) gives $\sigma_y(x)$, the deviation of the beam displacement. It is plotted against x to show a statistical beam displacement envelope in figures 19 and 20. In all plots, only the first three modes are considered and the coefficient of damping ζ_n for all modes is taken as 1%. In figures 19 and 20, the vibration is being minimized from $0 \le x \le 1$ and from $3/4 \le x \le 1$, respectively. The first mode dominates the uncontrolled displacement envelope in figure 19, but this is hardly surprising since the relative dominance of the first mode was seen in figure 2. These results are similar to those realized before for harmonic excitation. Compared to the global minimum, better control was achieved in the region of minimization, at the cost of less control outside of the region of minimization.

The vibration of the beam over the interval of minimization is represented quantitatively by Ψ in equation (58). In figures 21 and 22, Ψ is plotted versus the position x_c of the controller. Perfect control is achieved for collocation of source and controller. When minimizing over the length of the beam in figure 21, the reduction in Ψ lessens as the controller position coincides with nodes of the second and third modes. This is a result of the requirement that each mode be minimized independently for global reduction of Ψ, and a mode cannot be controlled if it cannot be excited. The requirement to minimize the modes independently can be verified by substituting equation (46.3) in equation (58) to expand Ψ over the modes:

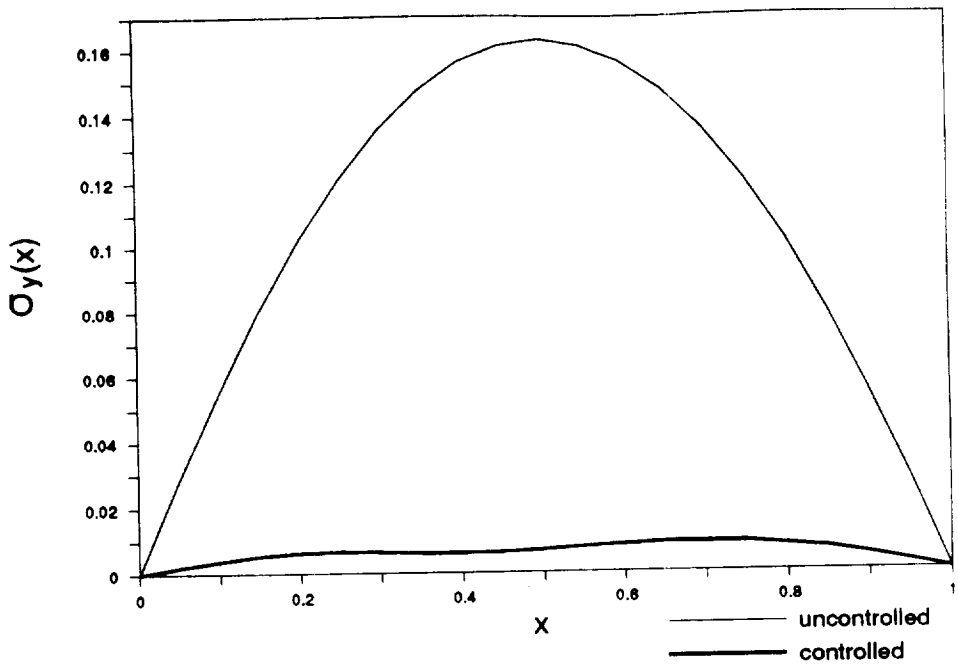

Figure 19. Deviation of beam displacement, $\sigma_y(x)$ before and after global control, $x_s = 1/6$, $x_c = 3/4$, $x_1 = 0$, $x_2 = 1$

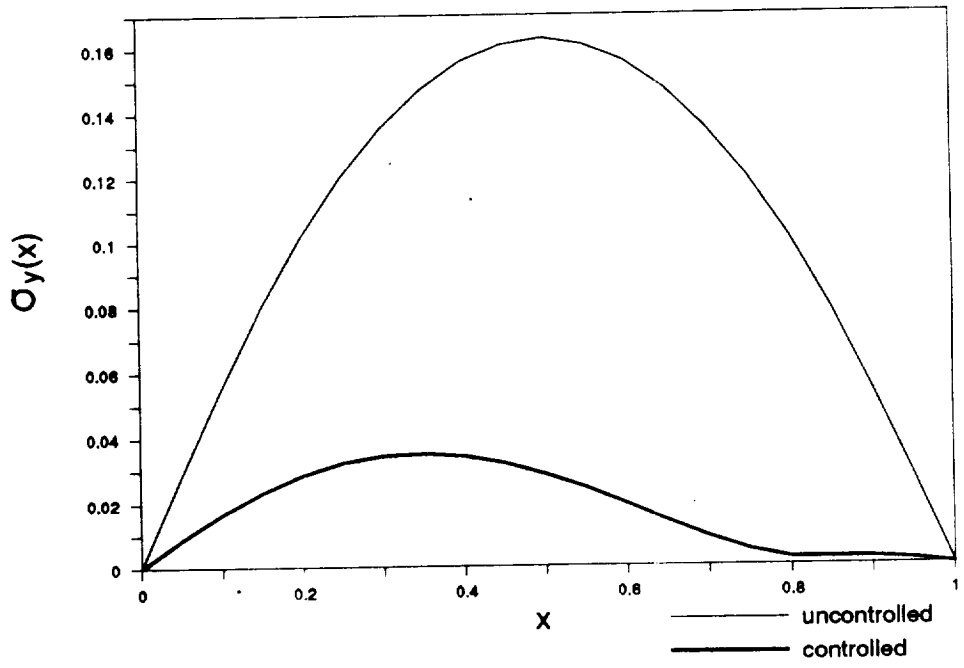

Figure 20. Deviation of beam displacement, $\sigma_y(x)$ before and after local control, $x_s = 1/6$, $x_c = 3/4$, $x_1 = 3/4$, $x_2 = 1$

$$\Psi = \frac{1}{4\pi} \sum_{n=1}^{\infty} \int_0^{\infty} d\omega |\, \hat{y}_n(\omega)\,|^2 \tag{61}$$

Even though the controller cannot control a mode that it cannot excite because of actuator location, it can still control the remaining modes, so figure 21 shows a minimum of 15 dB in the reduction of the cost function Ψ. This is quite different than what was observed in the case of harmonic excitation, where some controller location always existed for which no control was possible.

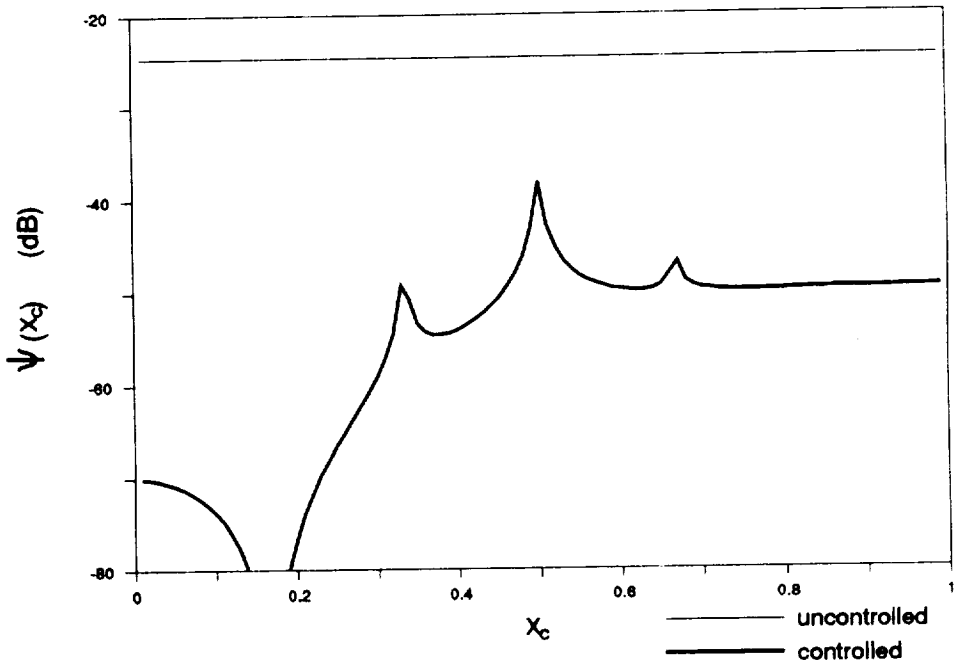

Figure 21. Effect of controller position x_c on global cost function Ψ, $x_s = 1/6$, $x_1 = 0$, $x_2 = 1$

When minimizing over a subinterval of the beam, figure 22 illustrates that locating the controller near a node can result in improved control. Figure 24 illustrates this improved control by plotting the deviation of the displacement after locating the controller at $x_c \approx .49$. Because of the modal coupling in a subinterval, the first and third modes are utilized to locally

control the second mode.

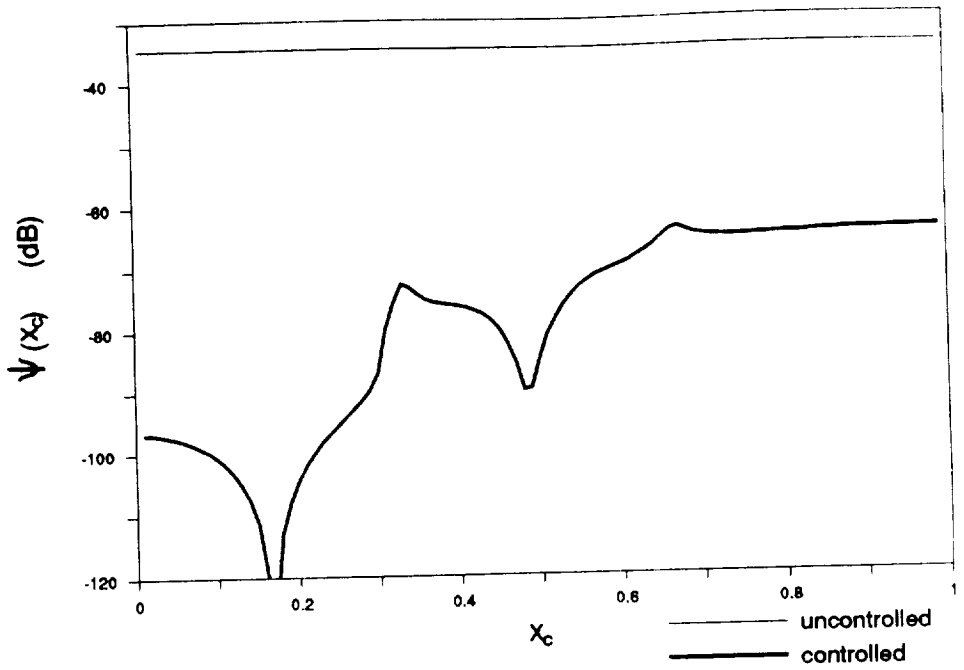

Figure 22. Effect of controller position x_c on local cost function Ψ, $x_s = 1/6$, $x_1 = 3/4$, $x_2 = 1$

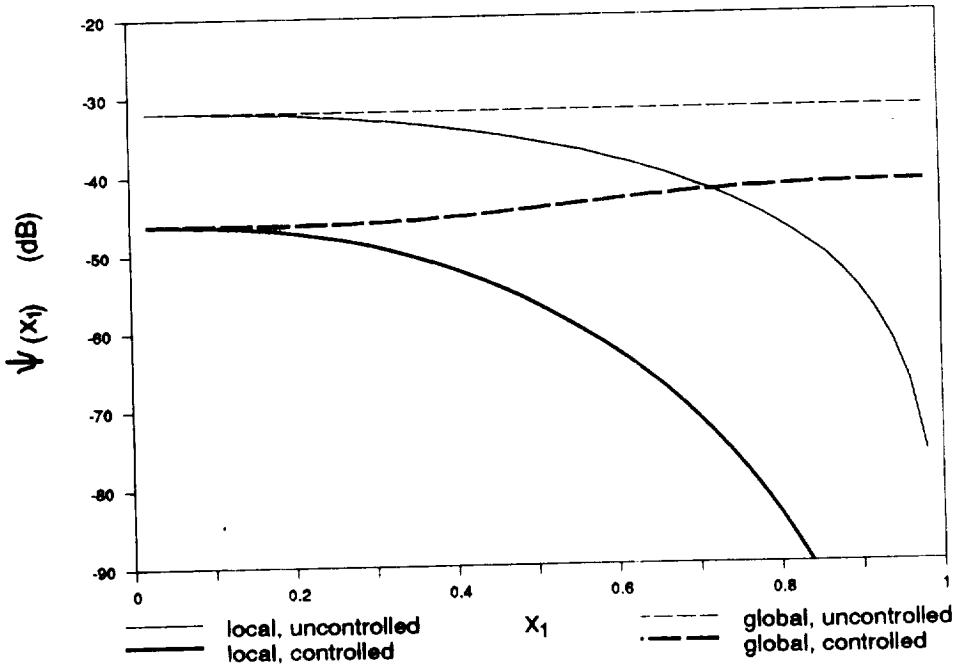

Figure 23. Effect of interval of minimization on both the local and global value of cost function Ψ before and after control, $x_s = 1/6$, $x_c = 3/4$, $x_2 = 1$

The effect of the interval of minimization on the reduction in Ψ is seen in figure 23. Greater control is possible as the interval of minimization is decreased. The global value of Ψ is also reduced when controlling locally for all values of the lower limit of minimization.

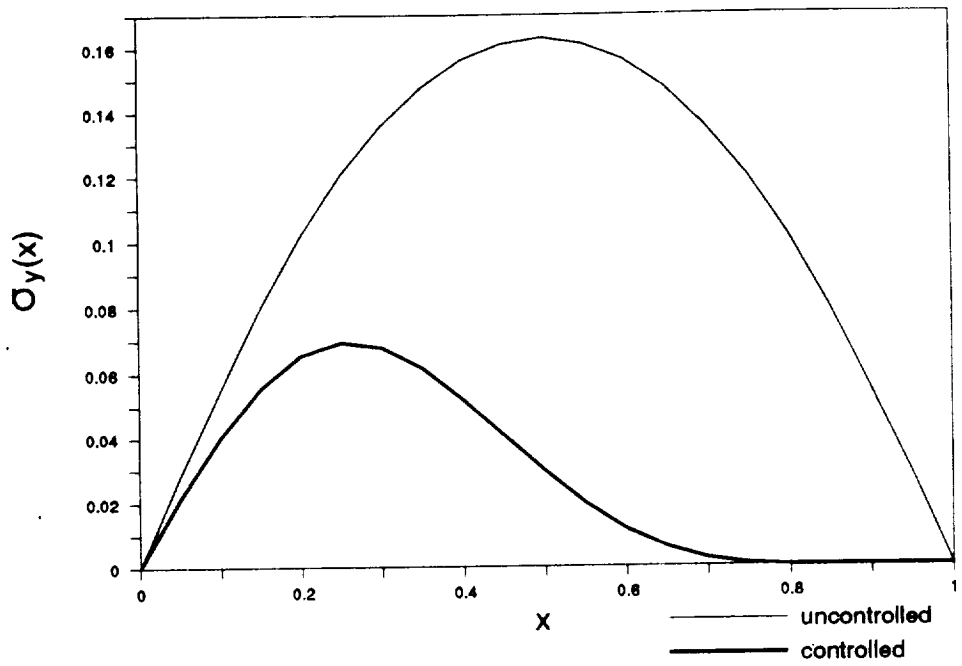

Figure 24. Deviation of beam displacement, $\sigma_y(x)$ after optimal placement of controller, $x_s = 1/6$, $x_c = .49$, $x_1 = 3/4$, $x_2 = 1$

The performance of the unconstrained controller has been examined, and it establishes that excellent control is possible over a broad frequency bandwidth for random noise excitation using only a single controller. Regardless of the interval of minimization, a reduction in the global beam vibration is always achieved. This differs from the results of chapter 3 where, for harmonic excitation, an increase was observed in global beam vibration when minimizing locally for certain arrangements of exciting frequency and controller location. The best location of the controller for global control was shown, in general, to be as near the exciting force as

possible, while avoiding node locations of the modes to be controlled because each must be controlled independently. When controlling locally, however, positioning the controller at a node location can result in improved control because of the local interference between the modes.

The controller was revealed to have the same transfer function as the controller used for harmonic excitation. This controller is not constrained by causality which may limit its use depending on the application, so a controller constrained by causality is also of interest. The discussion of the constrained random controller is taken further in appendix A.

Chapter 5

CONTROLLING TRANSIENT EXCITATION

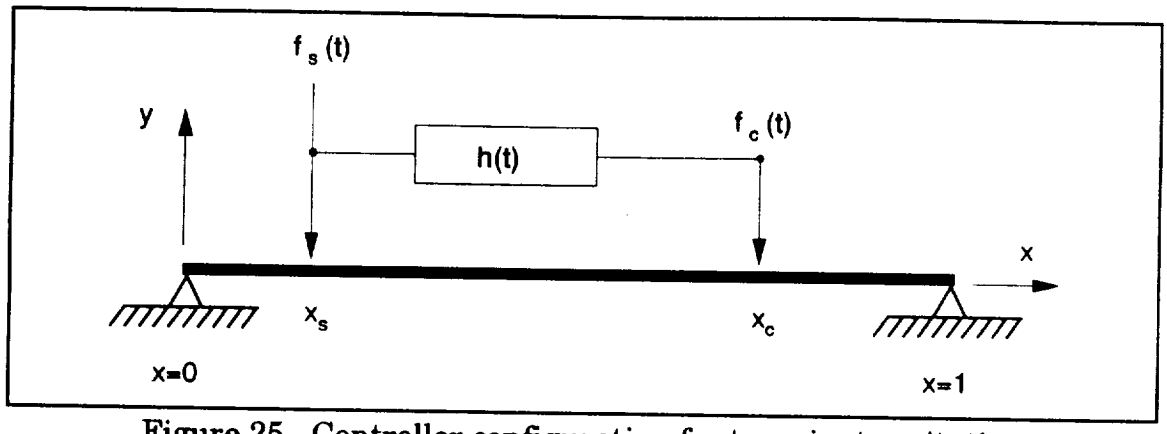

Figure 25. Controller configuration for transient excitation

In this chapter the force exciting the beam is assumed to be an impulse function. Two different controllers are used to control the resulting transient vibrations. The first controller uses one impulse delayed in time to minimize the vibrations, whereas the second controller uses two impulses, both delayed in time. The delays constrain the controller to be causal. The equations will be formulated for the two pulse controller, allowing the single pulse equations to be found by letting the amplitude of the second controlling pulse vanish.

The arrangement of the exciting and controlling forces is shown in figure 25. The primary source of excitation is represented by $f_s(t)$ and the secondary force, used for controlling the beam, by $f_c(t)$. For a single pulse excitation and two pulse control, these can be written

$$f_s(t) = f_{s0}\delta(t) \tag{69}$$

$$f_c(t) = f_{c1}\delta(t - t_1) + f_{c2}\delta(t - t_2) \qquad t_2 > t_1 \geq 0 \tag{70}$$

The linear relation between the exciting and controlling forces defines the controller. In the time domain this linear relation is written as

$$f_c(t) = \int_{-\infty}^{\infty} d\tau\, h(\tau) f_s(t - \tau) \tag{71}$$

where $h(t)$ is the impulse response of the controller. Substituting equations (69) and (70) into (71) gives

$$h(t) = h_1\delta(t - t_1) + h_2\delta(t - t_2) \tag{72}$$

where

$$h_1 = \frac{f_{c1}}{f_{s0}}$$

$$h_2 = \frac{f_{c2}}{f_{s0}} \tag{73}$$

The displacement of the beam due to a single exciting force is given by equation (17) where $h_s(x,t)$ is defined as the response of the beam at position x due to an impulse located at x_s. By superposition, the total displacement is

$$y(x,t) = \int_{-\infty}^{\infty} d\tau\, h_s(x,\tau) f_s(t - \tau) + \int_{-\infty}^{\infty} d\tau\, h_c(x,\tau) f_c(t - \tau) \tag{74}$$

where $h_c(x,t)$ is defined as the response of the beam at position x due to an impulse located at x_c. Using equations (69) and (70), this can be written,

$$y(x,t) = f_{s0}h_s(x,t) + f_{c1}h_c(x, t - t_1) + f_{c2}h_c(x, t - t_2) \tag{75}$$

Normalize by the amplitude of the exciting impulse by defining

$$y_8(x,t) \equiv \frac{y(x,t)}{f_{s0}} \tag{76}$$

which allows equation (75) to be written

$$y_8(x,t) = h_s(x,t) + h_1h_c(x, t - t_1) + h_2h_c(x, t - t_2) \tag{77}$$

In the case of a single pulse controller, h_2=0 and equation (77) is left with two degrees of freedom, h_1 and t_1. Similarly, the two pulse controller has four degrees of freedom. The four degrees of freedom will be reduced in the following analysis to three by letting the time between the two pulses be fixed at some positive constant α such that $\alpha = t_2 - t_1$.

A measure of the transient vibrations resulting from the initial impulse will be formed by squaring the displacement and integrating over all time. Integrating this quantity over some length of the beam results in a cost function to be minimized with respect to the impulse weights and delays of the controller. Define

$$\Lambda \equiv \int_{x_1}^{x_2} dx \int_0^{\infty} dt\, y^2(x,t) \tag{78}$$

To find Λ, first square equation (77):

$$\begin{aligned} y_\delta^2(x,t) = & h_s^2(x,t) + 2h_1 h_s(x,t) h_c(x,t-t_1) + 2h_2 h_s(x,t) h_c(x,t-t_2) \\ & + h_1^2 h_c^2(x,t-t_1) + 2h_1 h_2 h_c(x,t-t_1) h_c(x,t-t_2) + h_2^2 h_c^2(x,t-t_2) \end{aligned} \tag{79}$$

Substituting equation (79) into (78) gives the cost function to be minimized explicitly:

$$\Lambda = A_1 + 2h_1 A_2(t_1) + 2h_2 A_2(t_2) + h_1^2 A_3(t_1,t_1) + 2h_1 h_2 A_3(t_1,t_2) + h_2^2 A_3(t_2,t_2) \tag{80}$$

where

$$A_1 \equiv \int_{x_1}^{x_2} dx \int_0^{\infty} dt\, h_s^2(x,t)$$

$$A_2(\tau_1) \equiv \int_{x_1}^{x_2} dx \int_0^{\infty} dt\, h_s(x,t) h_c(x,t-\tau_1)$$

$$A_3(\tau_1,\tau_2) \equiv \int_{x_1}^{x_2} dx \int_0^{\infty} dt\, h_c(x,t-\tau_1) h_c(x,t-\tau_2) \tag{81}$$

It can easily be seen that the definitions in equations (81) are the same as those already defined by equations (54) where $A_1 = b_1(0)$, $A_2(\tau_1) = b_2(\tau_1)$, and $A_3(\tau_1, \tau_2) = b_3(\tau_2 - \tau_1) = b_3(\alpha)$. Now equation (80) may be written as

$$\Lambda = b_1(0) + 2h_1 b_2(t_1) + 2h_2 b_2(t_2) + h_1^2 b_3(0) + 2h_1 h_2 b_3(\alpha) + h_2^2 b_3(0) \tag{82}$$

To find the minimum value of the cost function Λ, calculate the partial derivatives with respect to the unknowns h_1, h_2, and t_1. Setting these derivatives equal to zero yields stationary points, which are necessary conditions for a minimum. The derivatives are

$$\frac{\partial \Lambda}{\partial h_1} = 2h_1 b_3(0) + 2h_2 b_3(\alpha) + 2b_2(t_1) \tag{83}$$

$$\frac{\partial \Lambda}{\partial h_2} = 2h_1 b_3(\alpha) + 2h_2 b_3(0) + 2b_2(t_2) \tag{84}$$

$$\frac{\partial \Lambda}{\partial t_1} = 2h_1 b'_2(t_1) + 2h_2 b'_2(t_2) - 2h_1 h_2 b'_3(\alpha) \tag{85}$$

Setting equations (83) and (84) equal to zero yields the linear system

$$\begin{bmatrix} b_3(0) & b_3(\alpha) \\ b_3(\alpha) & b_3(0) \end{bmatrix} \begin{Bmatrix} h_1 \\ h_2 \end{Bmatrix} = \begin{Bmatrix} -b_2(t_1) \\ -b_2(t_2) \end{Bmatrix} \tag{86}$$

which can be solved to give

$$h_1 = -\frac{b_2(t_1) b_3(0) - b_2(t_2) b_3(\alpha)}{b_3^2(0) - b_3^2(\alpha)} \tag{87}$$

$$h_2 = -\frac{b_2(t_2) b_3(0) - b_2(t_1) b_3(\alpha)}{b_3^2(0) - b_3^2(\alpha)} \tag{88}$$

After setting equation (85) equal to zero, equations (87) and (88) can be used to write a single equation in t_1 whose roots are stationary points of Λ. However, the equation is transcendental, with infinitely many roots. Moreover, it is not clear which root results in the global minimization of the

cost function Λ. An easy way around this problem is to substitute equations (87) and (88) into equation (82) to give Λ as a function of t_1 and then to graph the cost function so that the global minimum may be identified visually. This is done in figures 26 and 27.

In figure 26, the cost function Λ has been minimized over the entire length of the beam, or globally. Both the one and two pulse controller achieve their minimum values at nonzero delay times. The minimum for the one pulse controller is reached at $t_1 = T_1/2 \approx .318$, where T_1 is the period of the first eigenvalue, or eigenfrequency, of the beam, equal to $2/\pi \approx .637$. The delay times at which no control is possible for a single pulse controller correspond to the instants at which the energy in the first mode is all potential. Any attempt to control the beam with a single pulse at this instant only increases the energy in the first mode. It is possible to control the higher order modes at these instants, but spillover into the dominant first mode (see figure 2) prevents any reduction of the cost function.

To better illustrate this mechanism, consider a single degree of freedom spring mass system in an excited state. As the mass reaches the system equilibrium position its energy is purely kinetic and an impulse can be used to completely stop the subsequent motion. This is in contrast to the time at which the maximum displacement is reached and the energy of the system is purely potential. At this time, the best controlling pulse would be none at all, because striking the mass with an impulse can only serve to increase the energy in the system. The situation is more complicated for multiple degrees of freedom but the mechanisms are the same.

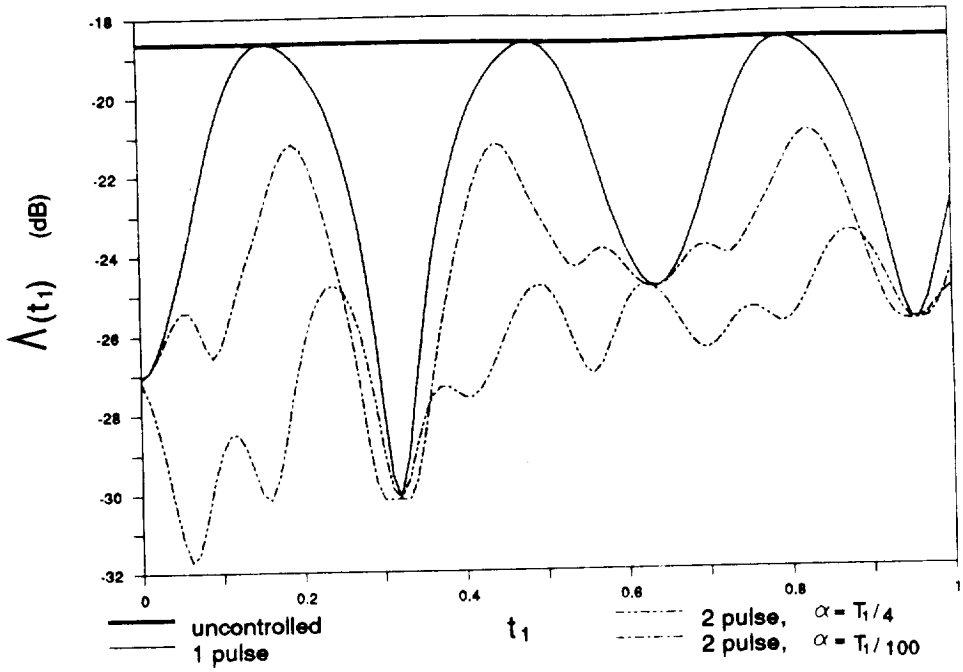

Figure 26. Cost function Λ vs. delay time t_1 of initial control impulse for global control, $x_s = 1/6$, $x_c = 3/4$, $x_1 = 0$, $x_2 = 1$

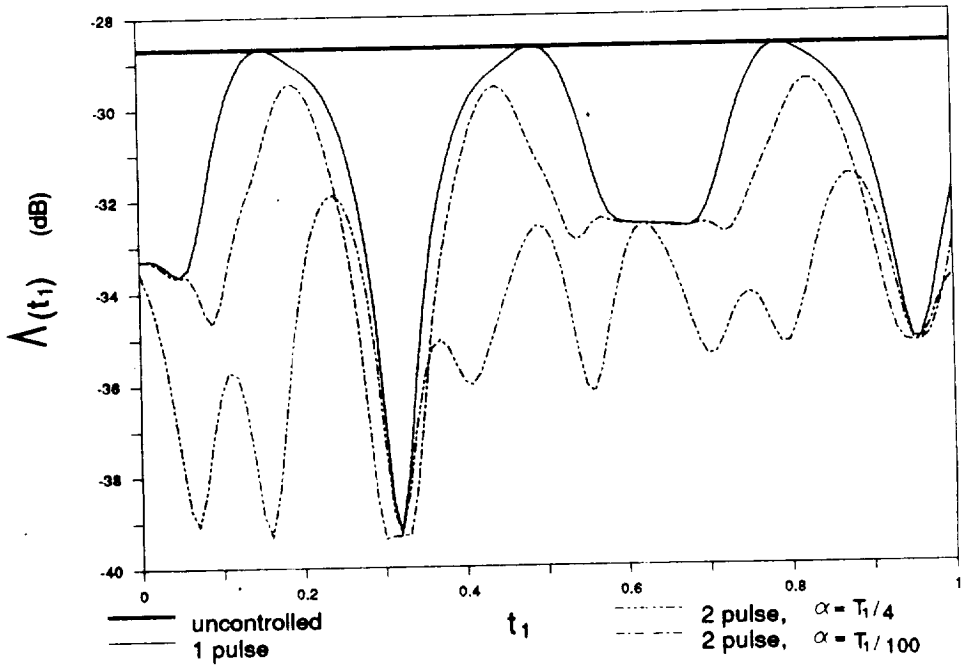

Figure 27. Cost function Λ vs. delay time t_1 of initial control impulse for local control, $x_s = 1/6$, $x_c = 3/4$, $x_1 = 3/4$, $x_2 = 1$

The single degree of freedom example in the last paragraph explains why the fundamental period of the oscillating cost functions in figures 26 and 27 are half the period of the first beam mode, but there are several other trends that can also be explained. One of these is the upward trend of the local minima for the cost functions. Recall that the plotted cost function is integrated over all time (see eqn. 78), but it is an impulse that is being controlled, so the major contribution to the integral comes from the time interval immediately following the exciting impulse. Thus, to minimize the cost function it is, in general, better not to delay control too long, because after the exciting impulse has decayed away, there is nothing left to control and the oscillating cost functions will have converged to the uncontrolled level.

Again looking at the single pulse control in figure 26, it is seen that the global minimum for Λ occurs at a delayed value for t_1 rather than a zero delay, and the fourth minimum results in better control than the third. It seems that waiting later can result in better control of the beam. This is true because of the interactions of the beam modes. The best delay at which to control is the delay at which the spillover from controlling the first mode helps control other modes as well. This phenomenon appears to be a strong function of the controller location as seen in figure 28, in which the optimal delay time t_1 for the global cost function is plotted against the controller location. The changes in optimal delay times are discrete jumps that occur when the controller location is such that the controller spillover couples with the beam modes in a way to make an alternate delay time more desirable.

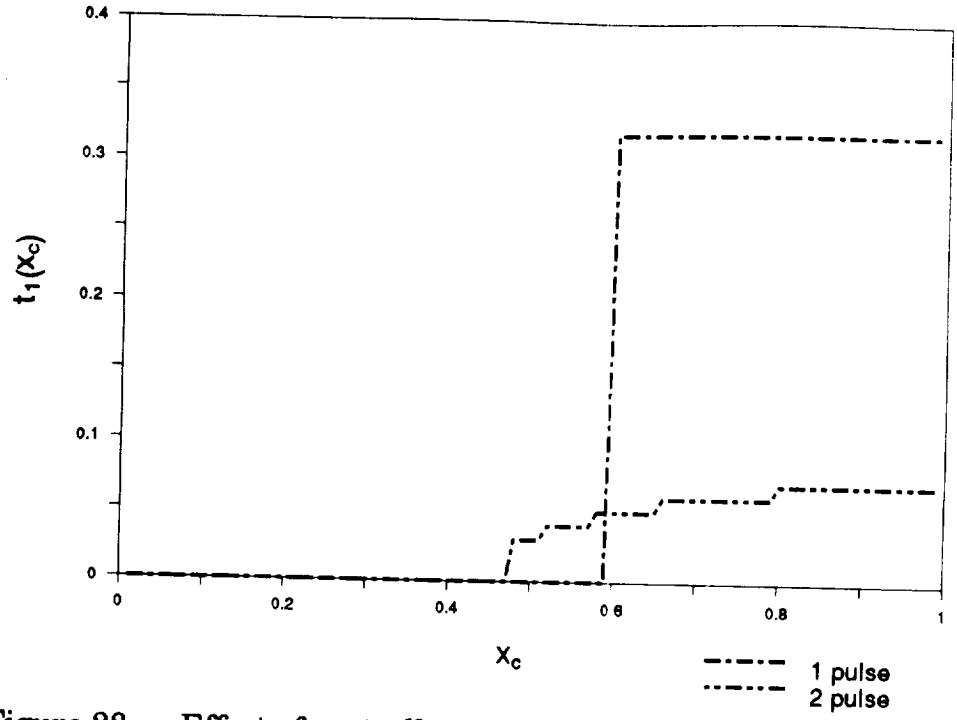

Figure 28. Effect of controller position on the optimal delay time for the controller, $x_s = 1/6$, $x_1 = 0$, $x_2 = 1$, $\alpha = T_1/4$

In contrast to the single pulse controller, the two pulse controller in figures 26 and 27 always results in some reduction of the cost function. This results from the controller being able to offset the spillover into the first mode with the second pulse while controlling higher order modes. The amount of control possible is highly dependent on the time α between the two pulses. For increasingly small values of α, the cost function ceases to show any noticeable changes after values smaller than $\alpha = T_1/100$, but better control is possible for greater choices of α. The increased complexity of the cost function for the two pulse controller will be discussed later.

It is worthwhile to comment on the similarity of figures 26 and 27 since some may be surprised that a global reduction would yield very nearly identical values of t_1 to minimize the cost function Λ. This is a result of the transient nature of the excitation. For transient excitation, no steady

opposition to a local disturbance can be developed. For this reason, the global and local minimizations yield very nearly the same results, as will be shown in later plots.

Now it is of interest to note the controller weights h_1 and h_2 that yield the control shown in figures 26 and 27. Figures 29 and 31 show these weights corresponding to the global control in figure 26, and figures 30 and 32 show those for the local control in figure 27. All of the weights oscillate with the period of the first beam mode.

For $\alpha = T_1/4$ in figures 29 and 30, the first weight of the two pulse controller is essentially the same as that of the single pulse controller; the second weight is the same also except that it is delayed by the time lag α between the control pulses. The peak values correspond to the optimal delay times in figures 26 and 27 and the zero crossings coincide with the delay times at which no control is possible.

The amplitude h_1 of the single pulse controller at $t_1 = 0$ can be largely attributed to the effect of the excitation source and controller locations on the first mode. To better see this, assume the beam is represented by its first mode only. Minimizing the cost function Λ in equation (78) with respect to $h_1(t_1 = 0)$ results in $h_1 = \sin(\pi x_s)/\sin(\pi x_c)$. For the locations of source and controller in figure 29, $h_1 = \sin(\pi/6)/\sin(3\pi/4) = 1/\sqrt{2} \approx .707$. The actual value of .66 read from figure 29 is lower because there is more than one mode to control and stopping the first mode completely by letting $h_1 = -1/\sqrt{2}$ would result in spillover into the remaining modes, resulting in less than optimum control.

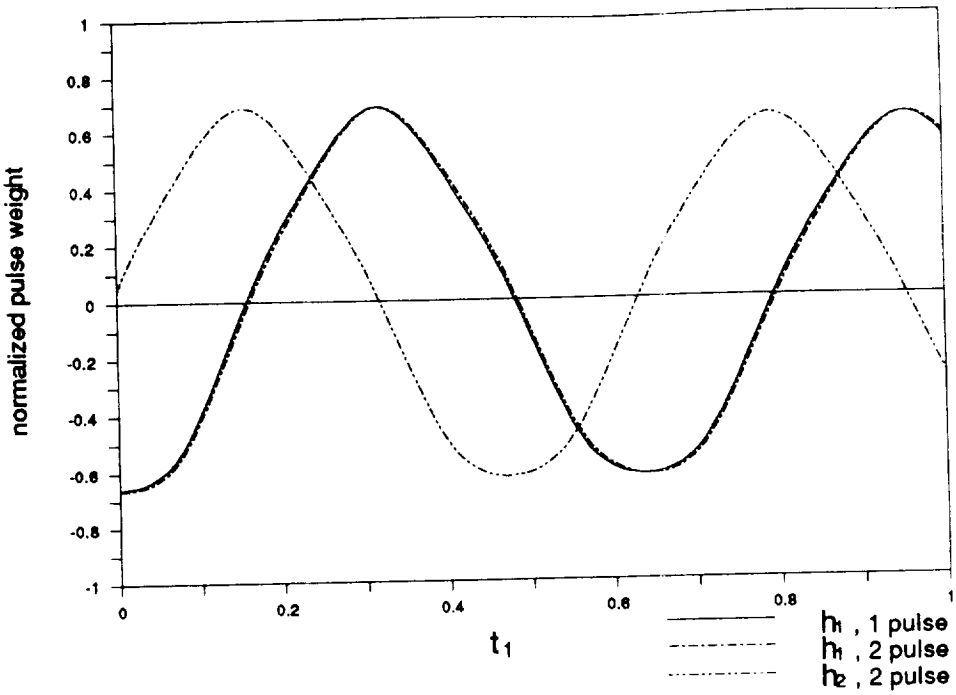

Figure 29. Weight of controller impulses for one and two pulse global controllers, $x_s = 1/6$, $x_c = 3/4$, $x_1 = 0$, $x_2 = 1$, $\alpha = T_1/4$

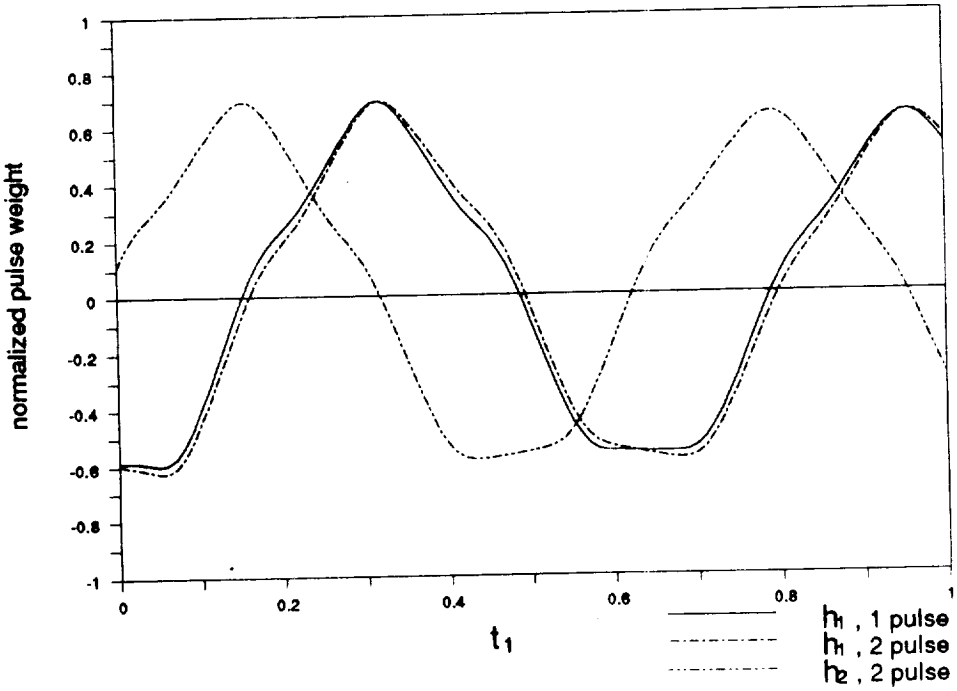

Figure 30. Weight of controller impulses for one and two pulse local controllers, $x_s = 1/6$, $x_c = 3/4$, $x_1 = 3/4$, $x_2 = 1$, $\alpha = T_1/4$

In view of the slight difference between figures 26 and 27, it is no surprise that figure 30 is very similar to figure 29. The increased importance of the higher order modes in figure 30 accounts for the increased distortion of the oscillating values of the weights.

Now look at the case in which the time α between the controlling pulses gets small. The weights become large and most often opposite in sign, as shown in figures 31 and 32 for $\alpha = T_1/100$. The "dipole" nature of the pulses allows control of higher order modes while limiting spillover in the first mode. The peak values in these figures indicate the delays at which the single pulse controller could not achieve any control. This two pulse controller does achieve some control (less than 3 dB globally) at these peaks as seen in figures 26 and 27, but larger control pulse weights are needed. The magnitudes of these pulse weights will be associated with the effort of the controller and are given in figures 31 and 32. The amplitudes are over ten times the amplitudes for more widely spaced controlling pulses that not only need much less effort but result in better control as well.

The best control results near the zero crossings of the weights in figures 31 and 32. Here the two weights sum to that of the single controller as given in figures 29 and 30. This agrees with the results seen in figures 26 and 27, where all configurations of one and two pulse controllers gave identical performance at the value $t_1 = T_1/2$. Thus, in return for somewhat increased performance over a single controller pulse, the two pulse controller requires significantly more effort if $\alpha \ll 1$.

Figure 26 showed a large change in the optimum delay time t_1 of the two pulse controller when the time α between the control pulses was changed. To

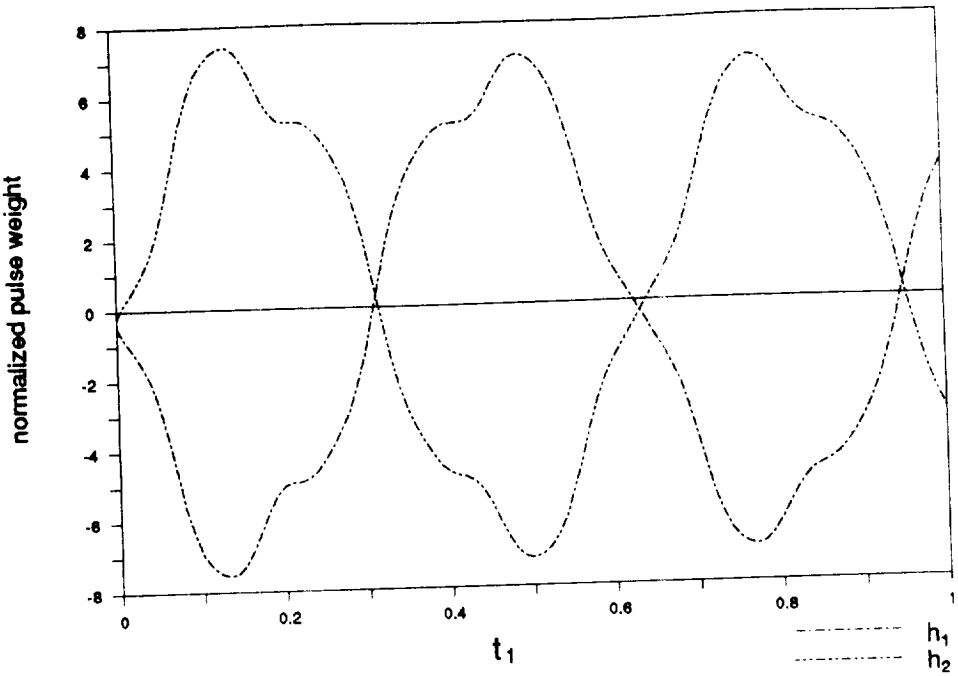

Figure 31. Weight of controller impulses for two pulse global controller, $x_s = 1/6$, $x_c = 3/4$, $x_1 = 0$, $x_2 = 1$, $\alpha = T_1/100$

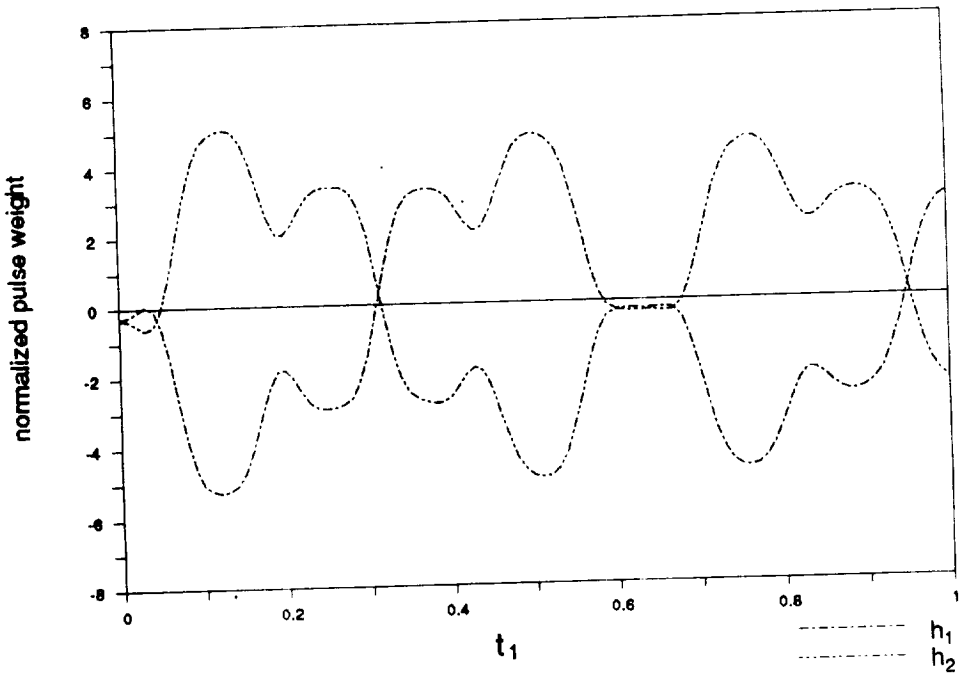

Figure 32. Weight of controller impulses for two pulse local controller, $x_s = 1/6$, $x_c = 3/4$, $x_1 = 3/4$, $x_2 = 1$, $\alpha = T_1/100$

better exhibit this relationship, a contour plot of the reduction in the cost function Λ is shown in figures 33 and 34 with t_1 and α as independent variables. For $\alpha = 0$, the determinant of the linear system in equation (86) is zero because $t_1 = t_2$, so results for the single-pulse controller are plotted along the ordinate for this degenerate case.

There is more to be seen in figures 33 and 34 than that they are complex and contain many local minima for Λ. Both figures contain strong contour lines that can be explained with the help of figures 26 and 27. The diagonal contours are centered about the two lines, $t_1 + \alpha = T_1/2$ and $t_1 + \alpha = 3T_1/2$, which correspond either to the first or second pulse acting at the minima seen in figures 26 and 27 for the single pulse controller. The strong vertical contours are located about the lines $t_1 = T_1/2$ and $t_1 = 3T_1/2$ which again correspond to the minima seen in figures 26 and 27. Along these contours, the second pulse has virtually no impact at all, indicating that its amplitude must be near zero. The global minima in figures 33 and 34 occur near the origin and show a reduction in the cost function Λ of more than 16 dB both globally and locally. The minima of Λ are at $(t_1, \alpha) \approx (.06, .12)$, and $(t_1, \alpha) \approx (.07, .11)$ in figures 33 and 34, respectively. The location of the minimum is caused by an interaction between the modes. Note the general spreading of the contour lines as t_1 and α increase. This can be understood by recalling again that the cost function Λ is obtained by integrating over time, so that, in general, the longer the controller delays the controlling pulses, the less reduction is possible.

Recall that the contours in figures 33 and 34 are functions of the controller configuration. To study the effect of controller location and interval of minimization, it would be necessary to regenerate and search contours such as figures 33 and 34, for each individual location of the

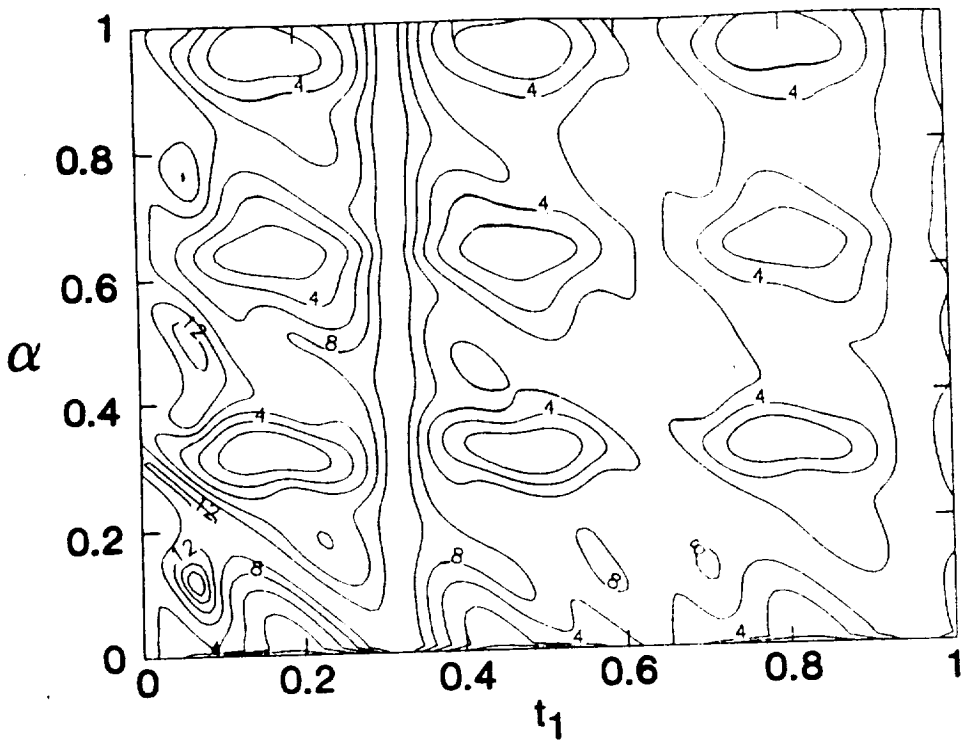

Figure 33. Decibels reduction in the global cost function $\Lambda(t_1, \alpha)$, $x_s = 1/6$, $x_c = 3/4$, $x_1 = 0$, $x_2 = 1$

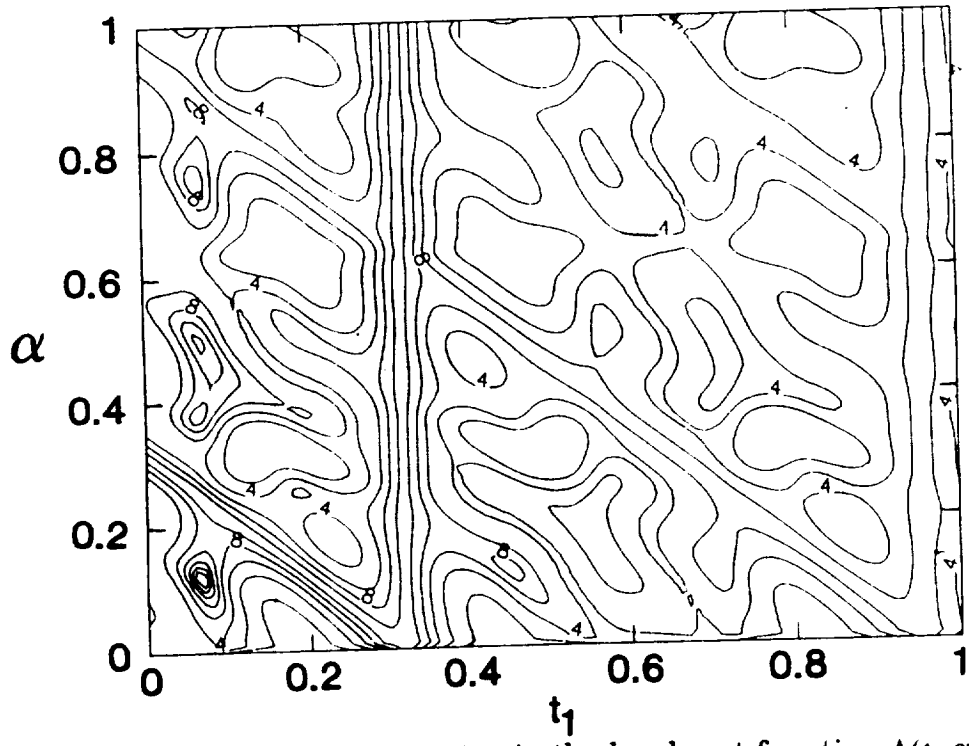

Figure 34. Decibels reduction in the local cost function $\Lambda(t_1, \alpha)$, $x_s = 1/6$, $x_c = 3/4$, $x_1 = 3/4$, $x_2 = 1$

controller and interval of minimization, so that the values of t_1 and α that result in global reduction of the cost function Λ would be found. Because this is time consuming, α is held fixed in figures 35-39, and the optimum t_1 sought along the line $\alpha = \alpha_{fixed}$. One should keep in mind though, that the quantitative control is also a function of the time α between control pulses.

Figures 35 and 36 show how the location of the controller affects the quantitative control. Just as in the case of controlling a harmonic exciting source in chapter 3, collocation of source and controller results in perfect control. It can be seen from figures 35 and 36 that substantial control is possible for any location of the controller in the case of global minimization of Λ, but, in general, it is best to move the controller as close as possible to the exciting source. Again a very subtle difference is seen between the shape of the global and local curves. This is seen throughout the plots in this chapter and reinforces the earlier statement that minimizing Λ locally in the case of transient excitation also results in very nearly a global minimum as well.

Now that the effect of controller location on Λ has been illustrated, it is of interest to see at what effort the control was gained. The effort can be seen by examining the weights h_1 and h_2 of the control pulses. The weights corresponding to the global control in figure 35 are shown in figure 37 and the weights corresponding to the local control in figure 36 are shown in figure 38. When the controller location nears the ends of the beam, the weights get large because poor modal coupling makes it increasingly difficult to excite the beam modes. The sudden changes in magnitude of the weights is due to a change in the optimum delay time t_1 for the initial controlling pulse. These jumps were seen earlier in figure 28. As the controller position is changed,

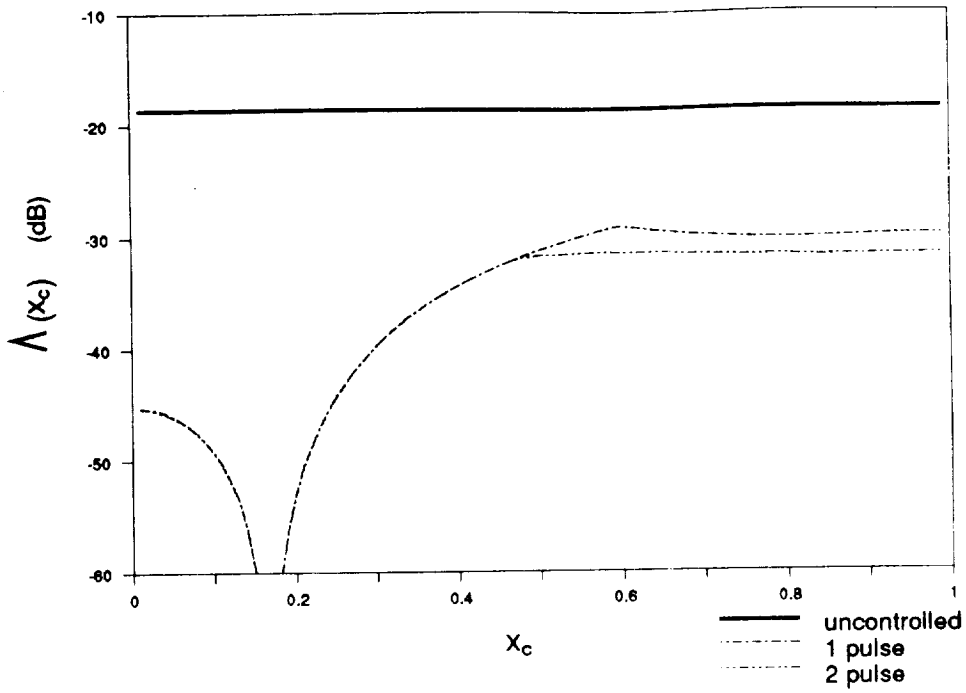

Figure 35. Effect of controller position on global cost function Λ, $x_s = 1/6$, $x_1 = 0$, $x_2 = 1$, $\alpha = T_1/4$

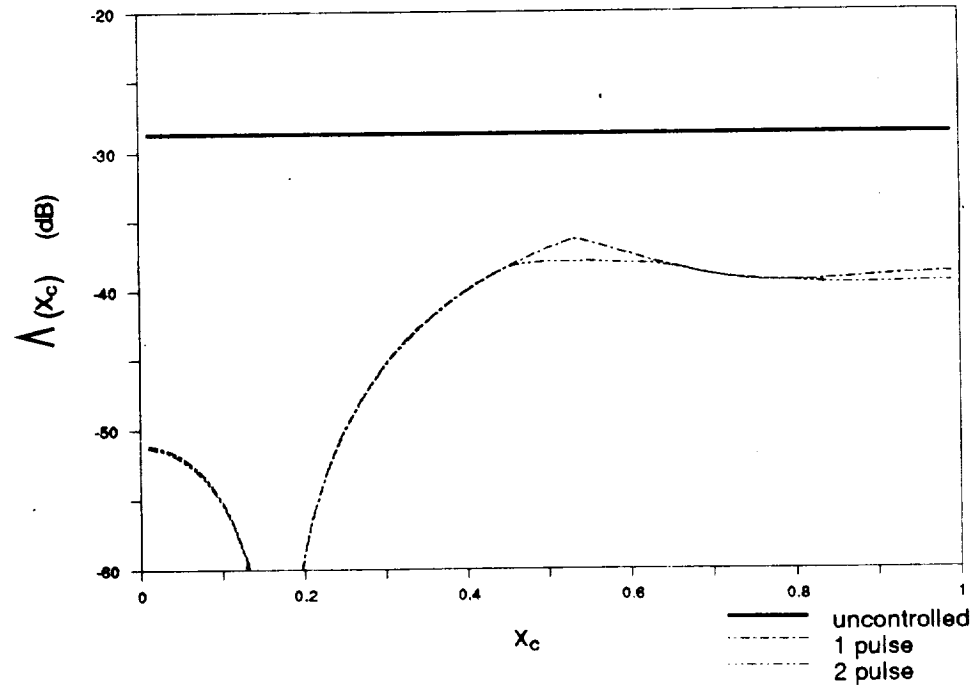

Figure 36. Effect of controller position on local cost function Λ, $x_s = 1/6$, $x_1 = 3/4$, $x_2 = 1$ $\alpha = T_1/4$

the optimum value for t_1 will change in discrete jumps. Correspondingly, the weight of the controller pulses will also change in discrete jumps. The sign change of the single pulse controller results from the change in sign of the modal eigenfunctions as the controller location changes. The second mode dominates this change in sign, which causes the jump to be near $x = 1/2$ which is the location of the sign change for the second modeshape. When either of the two weights h_1 or h_2 equals zero, there is no advantage to using a two pulse controller. These regions match the regions in figures 35 and 36 where no further reduction in the cost function Λ was possible with the two pulse controller.

The consequence of changing the controller location x_c was seen in figures 35 and 36. The location x_c has a major impact on the amount of control possible. Figure 39 shows that changing the interval of minimization does not have any dramatic results on the amount of control possible.

The effect of changing the controller location, interval of minimization, delay time of the controlling pulses, and the time between the control pulses have been observed. The performance was measured by the reduction in the cost function Λ. Recall that Λ is integrated over time and the interval of minimization. To better understand physically how the cost function is being reduced, define a spatial energy density function such that

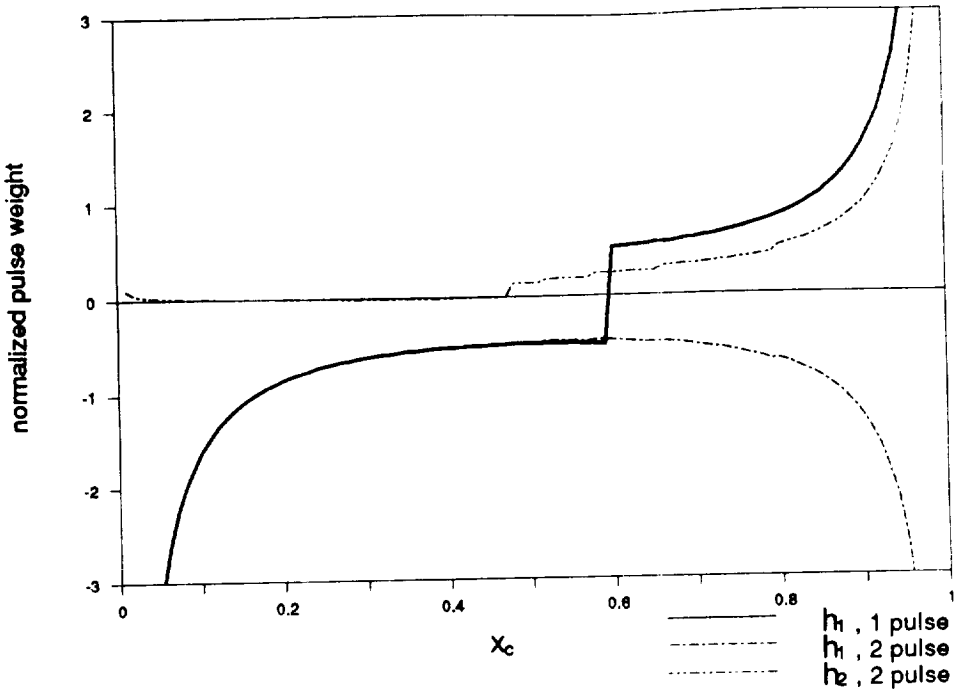

Figure 37. Effect of controller position on weight of control pulses for global control, $x_s = 1/6$, $x_1 = 0$, $x_2 = 1$, $\alpha = T_1/4$

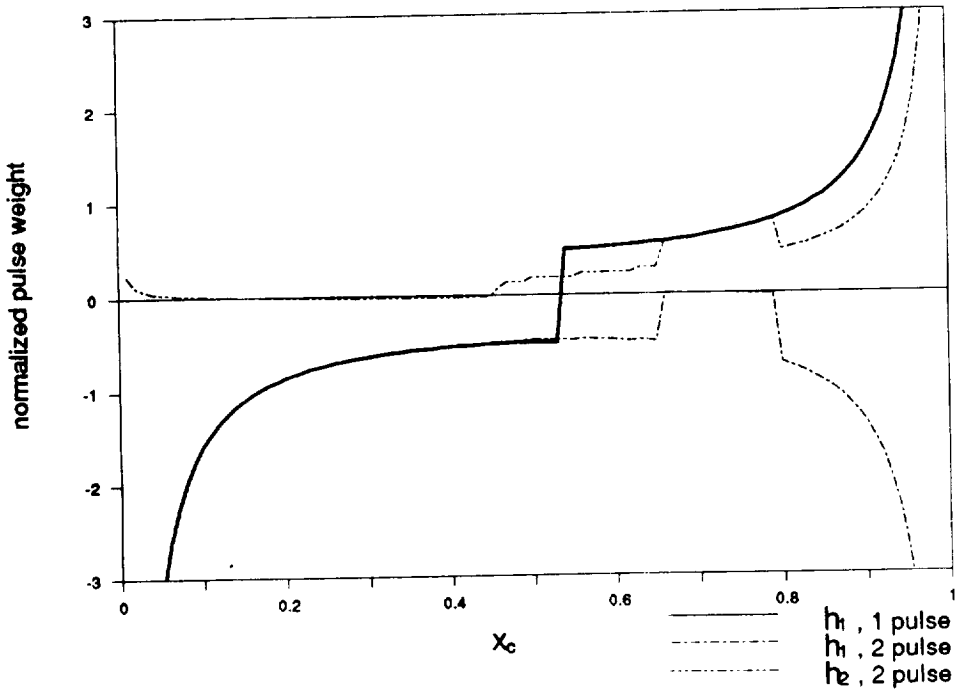

Figure 38. Effect of controller position on weight of control pulses for local control, $x_s = 1/6$, $x_1 = 3/4$, $x_2 = 1$ $\alpha = T_1/4$

$$\Lambda = \int_{x_1}^{x_2} dx\, E_y(x) \tag{89}$$

where

$$E_y(x) \equiv \int_0^{\infty} dt\, y^2(x,t) \tag{90}$$

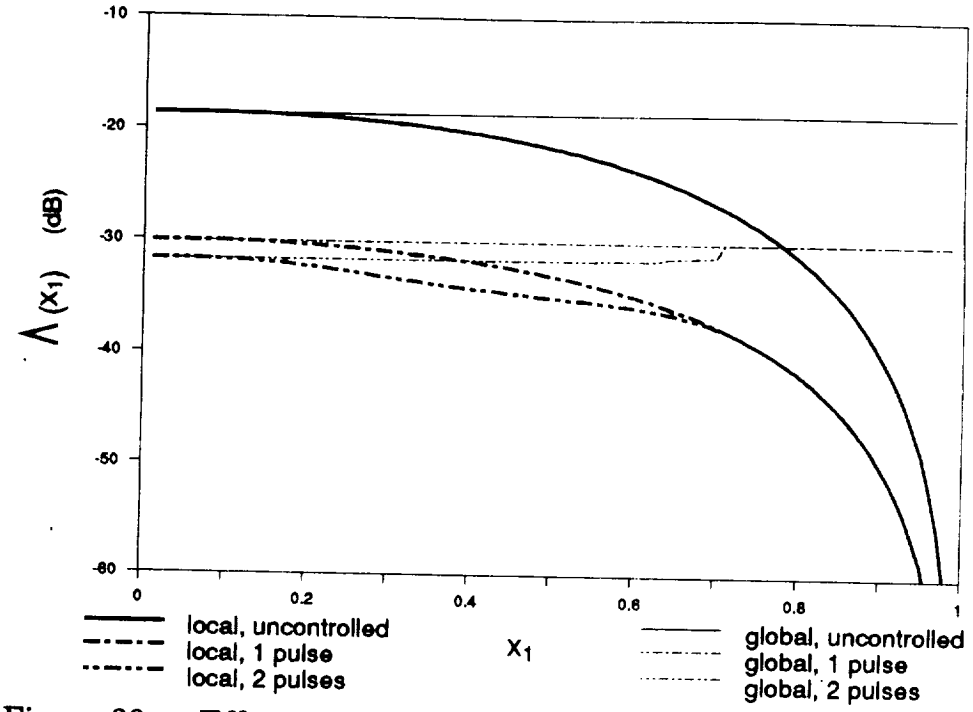

Figure 39. Effect of interval of minimization on cost function Λ, $x_s = 1/6$, $x_c = 3/4$, $x_2 = 1$, $\alpha = T_1/4$

The function $E_y(x)$ shows where on the beam the reduction in the cost function Λ is taking place. It is plotted in figure 40 for both global and local control by the one and two pulse controllers. The delay times t_1 and α in these plots are the optimal values as selected from figures 33 and 34.

The plots for the single pulse controller overlay one another and are indistinguishable. The interval of minimization has virtually no effect on the control possible by a single pulse. Looking back at figure 39 confirms that, regardless of the interval of minimization, the same global control is achieved

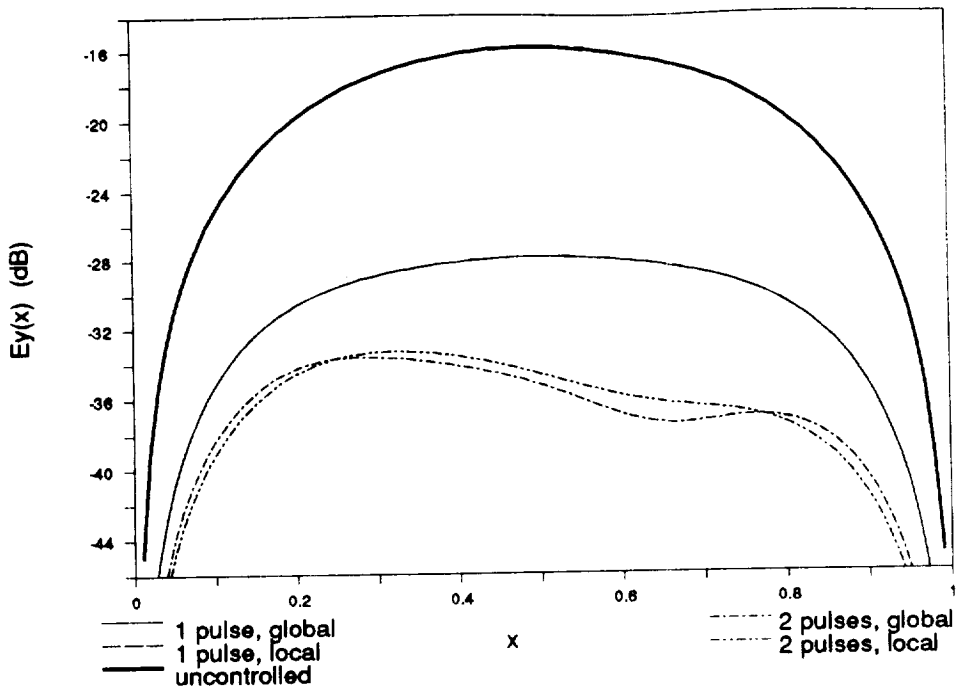

Figure 40. Spatial distribution of cost function Λ before and after control, $x_s = 1/6$, $x_c = 3/4$, local{$x_1 = 3/4$, $x_2 = 1$, 1 pulse($t_1 = T_1/2$), 2 pulse($t_1 = .07$, $\alpha = .11$)}, global{$x_1 = 0$, $x_2 = 1$, 1 pulse($t_1 = T_1/2$), 2 pulse($t_1 = .06$, $\alpha = .12$)}

with a single pulse controller. This is not true of the two pulse controller. It gives better control in the interval of minimization at the cost of giving up some control outside the interval.

From figure 40 one gains a feel for the location on the beam at which the cost function is being reduced. A more physical demonstration of how the two pulse controller achieves better control than the single pulse controller is evident in figures 41 and 42. These show time histories of the beam displacement $y(x,t)$ at a single position on the beam before and after control. The two pulse controller again uses the optimal values for t_1 and α as selected from figures 33 and 34.

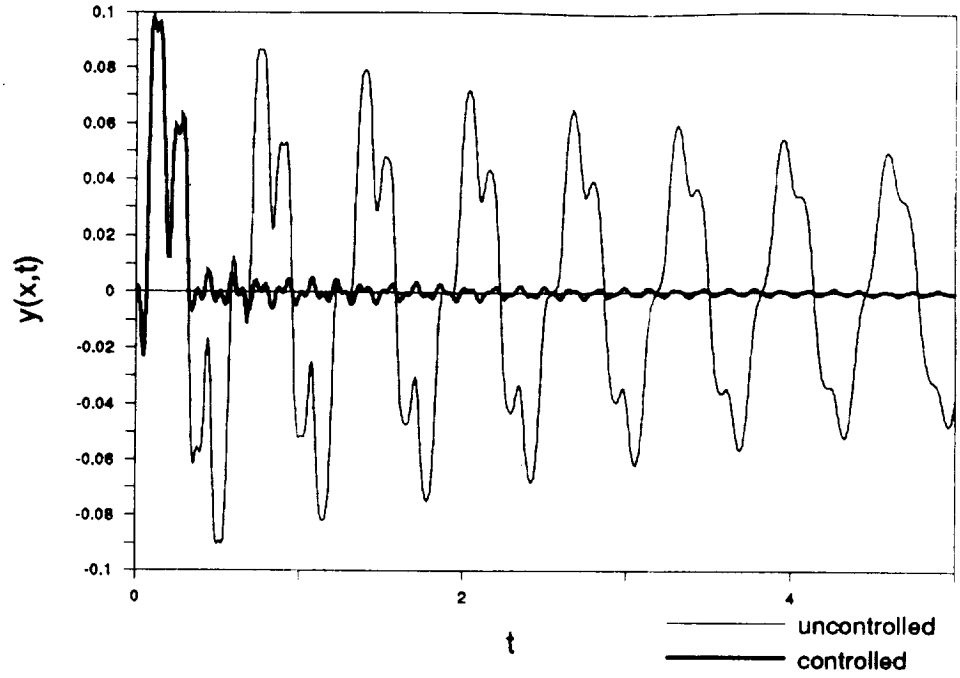

Figure 41. Time response of beam before and after control at position $x = 3/4$ using a single pulse controller, $x_s = 1/6$, $x_1 = 0$, $x_2 = 1$, $t_1 = T_1/2$

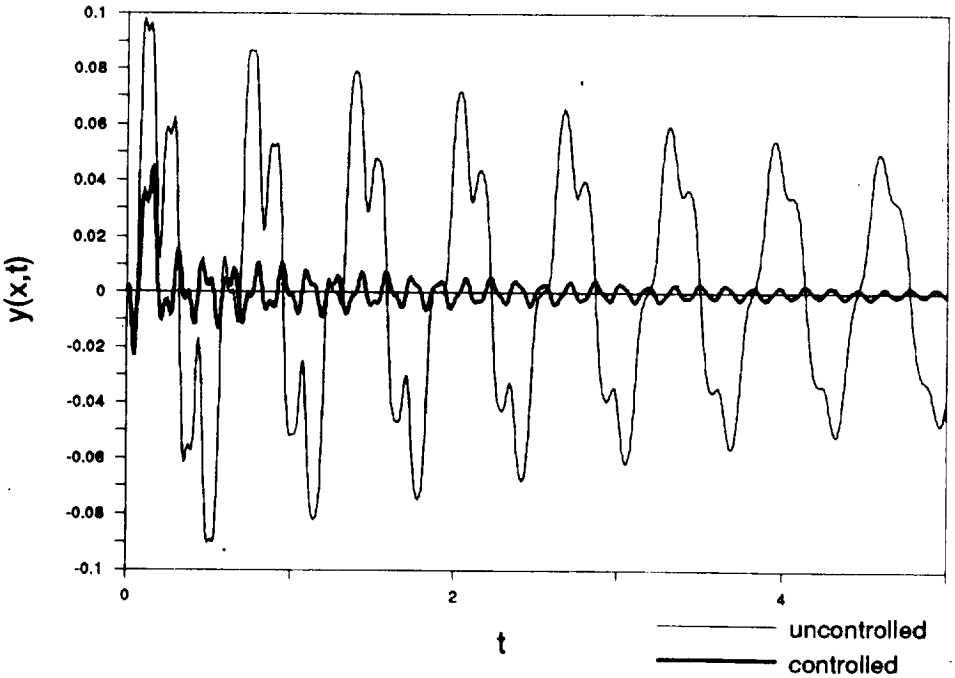

Figure 42. Time response of beam before and after control at position $x = 3/4$ using a two pulse controller, $x_s = 1/6$, $x_1 = 3/4$, $x_2 = 1$, $t_1 = .06$, $\alpha = .12$

Figure 41 gives the displacement before and after a single pulse controller is used. The before and after control plots are identical until the controller strikes at delay time t_1. The first mode is virtually eliminated from the time response after application of the controller. Notice the delay of the controller corresponds to $t_1 = T_1/2$ which is a time of zero displacement of the first order mode. At this instant the energy in the first mode is entirely kinetic which, as mentioned in the discussion of figures 26 and 27, marks the best time to strike the beam with a controlling impulse since the first mode dominates the displacement.

The two pulse controller in figure 42 strikes sooner than the single pulse controller in figure 41 in an attempt to reduce the displacement of the first beam mode in its initial half cycle. This is accomplished, but at the cost of slightly increased oscillations following the control pulses as compared to the single pulse controller.

In summary, it is always possible to control the transient vibration of the beam with both one and two impulses. The two impulse controller results in increased performance, as seen in figure 40, but at the cost of increased effort in the determination of the delay time and weight of the second pulse. To make the weight of the second pulse simple to determine, the time α between the pulses can be fixed as it was for most figures in this chapter but this offers only a slight improvement over the single pulse controller. Thus, for the two pulse controller to offer significant improvement, as was the case in figure 40, it is necessary to find the optimal delays for the first and second pulse independently. This is a point of difficulty for this method. Roots of a transcendental equation yield infinitely many choices for the delays t_1 and α

that result in stationary points of the cost function Λ, but there is no clear method for quickly determining the values of t_1 and α that result in the global minimum.

Chapter 6

SUMMARY

A controller to optimally reduce the vibration of a finite beam has been found for each of the three cases of excitation considered. For each controller, the performance was illustrated for a variety of configurations and the important results will now be summarized.

For harmonic excitation the optimal controller is seen to have two degrees of freedom, the amplitude of the controlling force and its phase relative to the exciting force. When minimizing the vibration globally, however, the only degree of freedom of the controller is the amplitude of the controlling force, because the orthogonality of the modes requires that each mode be minimized independently. Perfect control is possible at any single point on the beam, but when minimizing the vibration over some length of the beam, the only way to achieve perfect control is to collocate the excitation source and the control source. For separate locations, the best control exists when the excitation frequency is near resonance of one of the modes. Between the modal resonances, the quantitative control diminishes, until no control is possible at a discrete frequency which is a function of excitation location, controller location, and the interval of minimization. This was true when minimizing both locally and globally, but the frequency band in which the control was diminished, was much broader when minimizing globally. This bandwidth in which little control is achieved should not be a foremost concern though, because it always occurs at frequencies where the response of the beam is at a minimum and it is not as important to control the

vibration. The location of the controller should generally be as close as possible to the excitation source. For global control, avoid locating the controller at a node of a mode to be controlled; when controlling locally, locating the controller at a node of a contributing mode can be advantageous because controller spillover into that mode is eliminated.

For random excitation, the ideal controller was found to be the same controller that best minimizes the vibrations resulting from harmonic excitation. The performance of the random controller was then shown to be a frequency average of the performance of the harmonic controller, resulting in excellent control of random excitation using only a single controller. Perfect control is possible at any single point on the beam, but when minimizing the vibration over some length of the beam, the only way to achieve perfect control is to collocate the excitation source and the control source. The best location of the controller for global control was shown, in general, to be as near the exciting force as possible, while avoiding node locations of the modes to be controlled, because each mode must be controlled independently. When controlling locally, however, positioning the controller at a node location can result in improved control because of the coupling between the modes. Regardless of the interval of minimization, a reduction in the global beam vibration is always achieved. More control is gained as the interval of minimization is reduced, but not at the cost of increasing the global energy.

For transient excitation, two different controllers were found and compared. The first controller used a single impulse delayed in time to minimize the vibrations, whereas the second controller used two impulses, both delayed in time. The delays constrain the controller to be causal. If the time between successive pulses was fixed for the two pulse controller, it

resulted in virtually no improvement over the single pulse controller. The transient nature of the excitation prevents the controller from being able to zero the vibrations at a single point on the beam as was possible for steady-state excitations. Perfect control is achieved if the excitation force and controlling force are collocated. Changing the interval of minimization had no effect on the single pulse controller, and only a slight effect on the two pulse controller; Both controllers exhibited excellent control over all intervals of minimization. The best location for the controller was again as close as possible to the excitation source.

The highlights on controlling beam vibrations resulting from three types of excitation have been presented. The study was by no means exhaustive, and there are several interesting topics that could be examined further as future research.

In the case of both harmonic and random excitation, the controller was found to be have the same acausal transfer function. To implement an acausal controller, future values of the excitation source are required. This is not a problem in the case of harmonic excitation, since all future values are exactly known, but exact future values of a random excitation are generally *not* available. This requires the practical constraint of causality to be imposed on the controller used in the case of random excitation. It would be interesting to find the transfer function of the optimal controller constrained by causality and to compare its performance to the acausal controller in chapter 4 to see what is lost in performance as a result of the constraint.

It would also be useful to extend the theory of controlling a single transient pulse given in chapter 5 to control a sequence of random pulses. The controller need not be limited to only one or two control pulses. If many

pulses are used and the time between the control pulses is fixed, this problem is exactly a discretized version of that of finding the optimal controller constrained by causality for random excitation mentioned previously.

Also it would be desirable to implement and verify the controllers found in this work digitally in an experimental arrangement. It is not necessary, though, to use the controllers found in this work. Adaptive controllers could be used to control the vibrations, and their performance compared with the theoretical limits presented in this thesis.

REFERENCES

1. *Proceeding of the Workshop on Applications of Distributed System theory to the Control of Large Space Structures*, Jet Propulsion Laboratory, July, 1982, NASA CR-173119, (1983).

2. *Proceedings of the 3rd IFAC Symposium on Control of Distributed Parameter Systems*, Laboratoire d'Automatique et d'Analye des Systemes, Toulouse, France, 1982.

3. *Proceedings of the 20th IEEE Conference on Decision and Control*, San Diego, Calif., IEEE, New York, 1981.

4. "Dynamics and Control of Large Flexible Spacecraft", *Proceedings of the Third AIAA Symposium* held in Blacksburg, VA, June, 1981.

5. "Dynamics and Control of Large Flexible Spacecraft", *Proceedings of the Second AIAA Symposium* held in Blacksburg, VA, June, 1979.

6. "Dynamics and Control of Large Flexible Spacecraft", *Proceedings of the First AIAA Symposium* held in Blacksburg, VA, June, 1977.

7. Fattorini, H.O., "On Complete Controllability of Linear Systems", *Journal of Differential Equations*, Vol. 3, pp. 391-402, 1967.

8. Slemrod, Marshall, "A Note on Complete Controllability and Stabilizability for Linear Control Systems in Hilbert Space", *SIAM Journal of Control*, Vol. 12, No.3, August 1974.

9. Gonidou, Luc-Oliver, "Active Control of Flexural Power Flow in Elastic Thin Beams", *Virginia Polytechnic University Thesis*, February, 1988.

10. Meirovitch, L. and Bennighof, J.K., "Modal Control of Traveling Waves in Flexible Structures", *Journal of Sound and Vibration* (1986) 111(1), pp. 131-144.

11. von Flotow, A.H., "Travelling Wave Control for Large Spacecraft Structures", *Journal of Guidance, Control, and Dynamics*, Vol. 9, pp. 462-468, July-August, 1986.

12. Redman-White, W.; Nelson, P.A. and Curtis, A.R.D., "Experiments on the Active Control of Flexural Wave Power", *Journal of Sound and Vibration* 112(1), pp. 187-191, 1987.

13. Balas, M., "Active Control of Flexible Systems", *Journal of Optimization Theory and Applications*, Vol. 25, No. 3, 1978, pp. 415-436.

14. Meirovitch, L. and Baruh, H., "Control of Self-Adjoint Distributed-Parameter Systems", *AIAA 80-1707R* (1980).

15. Meirovitch, L. and Silverberg, L.M., "Active Vibration Suppression of a Cantilever Wing", *Journal of Sound and Vibration*, (1984), 97(3), pp. 489-498.

16. Thomson, William T., *Theory of Vibrations with Applications*, Prentice-Hall 1981.

17. Myint-U., Tyn, *Partial Differential Equations for Scientists and Engineers*, North-Holland 1987.

18. Herrick, D.; Canavin, J. and Strunce, R., "An Experimental Investigation of Modern Modal Control", *17th Aerospace Sciences Meeting*, New Orleans, La, January, 1979.

19. Hardin, Jay C., *Introduction to Time Series Analysis*, NASA Reference Publication 1145 (1986).

20. Widrow, Bernard, "Adaptive Noise Cancelling: Principles and Applications", *Proceedings of the IEEE*, Vol. 63, No. 12, pp. 1692-1716, December, 1975.

21. Elmore, W. and Heald, M., *Physics of Waves*, Dover, 1985

22. Fox, Charles, *An Introduction to the Calculus of Variations*, Oxford University Press 1950.

23. Krein, M.G., "Integral Equations on a Half-line with a Kernel Depending on the Difference of the Arguments", *American Mathematical Society Translations*, (2), 22 (1963), pp.163-288.

24. Macsyma, Symbolics, Inc., 257 Vassar Street, Cambridge, MA 02139.

25. Ludeman, Lonnie C., *Fundamentals of Digital Signal Processing*, Harper & Row 1986.

26. Kreyszig, Erwin, *Advanced Engineering Mathematics*, Wiley 1983.

27. Meirovitch, L., *Elements of Vibration Analysis*, Second Edition, McGraw-Hill, 1986.

28. Papoulis, A., *Probability, Random Variables, and Stochastic Processes*, McGraw-Hill, 1965.

29. Schäfer, Bernd E: and Holzach, Hans, "Experimental Research on Flexible Beam Modal Control", *German Aerospace Research Establishment (DFVLR)*, Oberpfaffenhofen, Federal Republic of Germany, 1985.

30. Dickerson, Stephen L. and Jarocki, George, "A Design Procedure for Active Control of Beam Vibrations", *Proceedings of the Workshop on Applications of Distributed System Theory to the Control of Large Space Structures*, NASA CR-173,119 (1983).

31. Williams, Jeffrey P., and Montgomery, Raymond C., "Simulation and Testing of Digital Control on a Flexible Beam", *AIAA Guidance and Control Conference*, August 9-11, 1982.

32. Camotim, D. and Roorda, J., "Active Vibration Control of a Simple Beam", *Transactions of the Canadian Society for Mechanical Engineering*, Vol. 7, No. 4, 1983.

33. Bernstein, Dennis S., and Rosen, I. Gary, "Finite-Dimensional Approximation for Optimal Fixed-Order Compensation of Distributed Parameter Systems", *NASA Contractor Report 181674*, June, 1988.

34. Palac, Donald T., "Analysis of Active Control of Cantilever Beam Bending Vibrations", *Air Force Institute of Technology Thesis*, AFIT/GA/AA/78D-6, December, 1978.

35. Hungerford, John B., "Active Control of Bending Vibration in a Cantilever Beam", *Air Force Institute of Technology Thesis*, AFIT/GA/AA/77D-7, 1977.

Appendix A

THOUGHTS ON CAUSAL CONTROL OF A STATIONARY RANDOM PROCESS

In chapter 4, an optimal controller was found to control white noise excitation. The disadvantage of the controller was that it was acausal and required future values of the noise excitation in order to be implemented. In some applications, a good estimate of future excitation values may exist, but for a completely general application, the controller for random excitation must be constrained to using only past values of the random noise excitation. Unfortunately, the constraint of causality makes the ideal controller considerably more difficult to find. The calculus of variations is employed here to find an integral equation that the constrained controller must satisfy. Both the analytical and numerical solution of this equation are then discussed.

Imposition of the constraint of causality is possible in both the frequency and time domains. In the frequency domain, causality causes the real and imaginary part of the transfer function to be dependent. If the real part is known, the imaginary part can be found by the relation[21]

$$I(\omega) = \frac{\omega}{\pi} \int_{-\infty}^{\infty} d\omega' \frac{R(\omega')}{\omega'^2 - \omega^2} \tag{A1}$$

One way to satisfy the constraint of causality is to let $H(\omega) = R(\omega) + jI(\omega)$ in equation (56), where $R(\omega)$ and $I(\omega)$ are the real and imaginary part of $H(\omega)$, respectively. Now use the integral relation in equation (A1) to get the cost functional Ψ in terms of only one independent function. This results in

$$\Psi = \frac{1}{2\pi}\int_{-\infty}^{\infty} d\omega B_1(\omega)$$
$$+\frac{1}{2\pi}\int_{-\infty}^{\infty} d\omega B_2^*(\omega)\left[R(\omega)+\frac{j\omega}{\pi}\int_{-\infty}^{\infty} d\omega' \frac{R(\omega')}{\omega'^2-\omega^2}\right]$$
$$+\frac{1}{2\pi}\int_{-\infty}^{\infty} d\omega B_2(\omega)\left[R(\omega)-\frac{j\omega}{\pi}\int_{-\infty}^{\infty} d\omega' \frac{R(\omega')}{\omega'^2-\omega^2}\right]$$
$$+\frac{1}{2\pi}\int_{-\infty}^{\infty} d\omega B_3(\omega)\left[R^2(\omega)+\frac{\omega^2}{\pi^2}\int_{-\infty}^{\infty} d\omega' d\omega'' \frac{R(\omega')R(\omega'')}{(\omega'^2-\omega^2)(\omega''^2-\omega^2)}\right]$$

which is a very complicated integral equation.

In the time domain, causality is more simply enforced by requiring $h(t)$, the impulse response of the controller, to be zero for $t < 0$. This affects the limits in equation (53) such that

$$\Psi = b_1(0) + 2\int_0^{\infty} d\tau h(\tau) b_2(\tau) + \int_0^{\infty} d\tau d\tau' h(\tau) b_3(\tau-\tau') h(\tau') \qquad \text{(A2)}$$

Now the problem is in the time domain rather than the frequency domain. Unfortunately, the quantity to minimize is still an integral equation, but not as complicated as was the frequency domain equation.

An impulse response function $h(t)$ is sought that will minimize Ψ, which is by definition, always a positive quantity. This is a problem in the calculus of variations[22]. If a minimum exists, a necessary condition is that it be at a stationary point of Ψ. Finding a stationary point is not sufficient however, to say that the point represents a minimum or maximum, but fortunately in many physically motivated problems, it will be obvious. If only one stationary point exists for Ψ, then it must be the minimum since a controller could always be chosen to make Ψ larger. To find a stationary point, first calculate the variation of Ψ in equation (A2) with respect to the controller

$h(\tau)$:

$$\delta\Psi = 2\int_{-\infty}^{\infty} d\tau\, b_2(\tau)\delta_\tau h + \int_{-\infty}^{\infty} d\tau d\tau' \{b_3(\tau-\tau')h(\tau')\delta_\tau h + b_3(\tau-\tau')h(\tau)\delta_\tau h\} \qquad \text{(A3)}$$

and rearrange to give

$$\delta\Psi = 2\int_{0}^{\infty} d\tau\, b_2(\tau)\delta_\tau h + \int_{0}^{\infty} d\tau d\tau' \{b_3(\tau-\tau') + b_3(\tau'-\tau)\} h(\tau')\delta_\tau h \qquad \text{(A4)}$$

Looking back at equation (54), $b_3(\tau)$ is

$$b_3(\tau) = \int_{-\infty}^{\infty} d\tau_1 \int_{x_1}^{x_2} dx\, h_c(x,\tau_1) h_c(x,\tau_1-\tau) \qquad \text{(A5)}$$

Now use $\tau_2 = \tau_1 - \tau$ to change the variable of integration resulting in

$$b_3(\tau) = \int_{-\infty}^{\infty} d\tau_2 \int_{x_1}^{x_2} dx\, h_c(x,\tau_2+\tau) h_c(x,\tau_2) \qquad \text{(A6)}$$

which, when compared with equation (A5), clearly reveals that $b_3(\tau) = b_3(-\tau)$. Because $b_3(\tau)$ is an even function, equation (A4) can be rewritten as

$$\delta\Psi = 2\int_{-\infty}^{\infty} d\tau \left\{ b_2(\tau) + \int_{0}^{\infty} d\tau'\, b_3(\tau-\tau')h(\tau') \right\} \delta_\tau h \qquad \text{(A7)}$$

A stationary point is defined by $\delta\Psi \equiv 0$. Since $\delta_\tau h$ is a function that can be chosen arbitrarily to prevent the integration from being zero, the integrand itself must everywhere be identically zero. This results in the Euler, or governing, equation:

$$b_2(\tau) + \int_{0}^{\infty} d\tau'\, b_3(\tau-\tau')h(\tau') = 0 \qquad \text{(A8)}$$

This particular integral equation is of a very common form known as the Wiener-Hopf integral equation. If the controller were not restricted to $t \geq 0$, it

could be solved by utilizing the convolution theorem of the Fourier transform which gives the same result as already found for the unconstrained random controller in chapter 4.

It may seem that the properties of the one-sided Laplace transform could be utilized to give

$$H(s) = -\frac{B_2(s)}{B_3(s)} \tag{A9}$$

but this is not possible since the convolution theorem is defined only for functions that are zero for $t < 0$; $b_3(\tau)$ is even, so the Laplace transform cannot be used. Of course the integral in equation (A8) could be separated into two one-sided integrals but then $h(\tau)$ is coupled with limits and an algebraic solution such as equation (A9) is not possible.

An analytical method for solving equation (A8), which requires the Fourier transform of the kernel $b_3(\tau)$ to be factored into two functions that are analytic in the left and right half-planes, respectively, is presented by Krein[23]. Factoring the product of two summations over the modes would be a very tedious process, but it may be possible to utilize a computer program that does symbolic manipulation, such as Macsyma[24], to aid in this task.

A straightforward approach to obtain a numerical solution is to discretize equation (A8) and solve the resulting simultaneous linear system of equations for discrete values of the desired controller function. Discretizing equation (A8) yields

$$b_2(k\Delta) + \Delta \sum_{n=0}^{N} b_3(k\Delta - n\Delta) h(n\Delta) = 0 \qquad k = 0, 1, \ldots, N \tag{A10}$$

The functions $b_2(\tau)$ and $b_3(\tau)$ are presented in closed form in appendix B. The solution to equation (A10) yields the impulse response of the controller. Substituting this into a discrete version of equation (A2) gives the approximate performance of the controller:

$$\Psi = b_1(0) + 2\Delta \sum_{n=0}^{N} h(n\Delta)b_2(n\Delta) + \Delta^2 \sum_{n=0}^{N}\sum_{k=0}^{N} h(n\Delta)b_3(n\Delta - k\Delta)h(k\Delta) \qquad \text{(A11)}$$

Unfortunately, the solution of the discrete system created questions rather than answers. The discrete values of the impulse response $h(t)$ had large oscillations at $t = 0$ and $t = N\Delta$. The oscillations became more tightly spaced and stronger as the stepsize Δ was decreased. Substituting the result into equation (A11) indicated a large reduction in the beam vibration. To check the reduction of displacement in the time domain, the beam equation was discretized and control simulated. After control, the amplitude of the displacement increased! If the oscillations were removed from the ends of the discrete impulse response, a reduction in displacement was observed. This would seem to indicate that the oscillations were not part of the actual solution, but if they were eliminated, then other problems occurred. As an example, minimizing the beam vibration globally did not reduce the global cost function as much as minimizing locally did. This makes absolutely no sense at all. This may be the result of the determinant of the system matrix rapidly approaching zero as N increases, although no thorough explanation could be found.

The problem of finding the optimal causal controller has been briefly discussed. This is a problem which contains many subtleties, and further research is necessary before these subtleties can be fully understood.

Appendix B

RELEVANT INTEGRALS

The closed form solution of several integrals is needed for plotting the solutions found in the text. The first is

$$S_{nm}(t_1,t_2)=\int_0^\infty d\tau\, h_n(\tau-t_1)h_m(\tau-t_2) \qquad t_2\geq t_1\geq 0$$

where

$$h_n(t)=\frac{1}{\omega_{d,n}}e^{-\omega_n\zeta_n t}\sin\omega_{d,n}t\,u_s(t)$$

This can be solved to give

$$\begin{aligned}S_{nm}(t_1,t_2)=b_{nm}\{&\cos\omega_{d,n}t_1\cos\omega_{d,m}t_2X_{nm}\\&-\cos\omega_{d,n}t_1\sin\omega_{d,m}t_2Y_{nm}\\&-\sin\omega_{d,n}t_1\cos\omega_{d,m}t_2Y_{mn}\\&+\sin\omega_{d,n}t_1\sin\omega_{d,m}t_2Z_{nm}\}\end{aligned}$$

where

$$b_{nm}=\frac{1}{\omega_{d,n}\omega_{d,m}}e^{-\omega_n\zeta_n(t_2-t_1)}$$

and

$$\begin{aligned}X_{nm}=&\frac{(\omega_{d,n}+\omega_{d,m})\sin(\omega_{d,n}+\omega_{d,m})t_2-(\omega_n\zeta_n+\omega_m\zeta_m)\cos(\omega_{d,n}+\omega_{d,m})t_2}{2\{(\omega_n\zeta_n+\omega_m\zeta_m)^2+(\omega_{d,n}+\omega_{d,m})^2\}}\\&-\frac{(\omega_{d,n}-\omega_{d,m})\sin(\omega_{d,n}-\omega_{d,m})t_2-(\omega_n\zeta_n+\omega_m\zeta_m)\cos(\omega_{d,n}-\omega_{d,m})t_2}{2\{(\omega_n\zeta_n+\omega_m\zeta_m)^2+(\omega_{d,n}-\omega_{d,m})^2\}}\end{aligned}$$

$$\begin{aligned}Y_{nm}=&\frac{(\omega_n\zeta_n+\omega_m\zeta_m)\sin(\omega_{d,n}-\omega_{d,m})t_2+(\omega_{d,n}-\omega_{d,m})\cos(\omega_{d,n}-\omega_{d,m})t_2}{2\{(\omega_n\zeta_n+\omega_m\zeta_m)^2+(\omega_{d,n}-\omega_{d,m})^2\}}\\&+\frac{(\omega_n\zeta_n+\omega_m\zeta_m)\sin(\omega_{d,n}+\omega_{d,m})t_2-(\omega_{d,n}+\omega_{d,m})\cos(\omega_{d,n}+\omega_{d,m})t_2}{2\{(\omega_n\zeta_n+\omega_m\zeta_m)^2+(\omega_{d,n}+\omega_{d,m})^2\}}\end{aligned}$$

$$Z_{nm} = -\frac{(\omega_{d,n} - \omega_{d,m})\sin(\omega_{d,n} - \omega_{d,m})t_2 - (\omega_n\zeta_n + \omega_m\zeta_m)\cos(\omega_{d,n} - \omega_{d,m})t_2}{2\{(\omega_n\zeta_n + \omega_m\zeta_m)^2 + (\omega_{d,n} - \omega_{d,m})^2\}}$$

$$-\frac{(\omega_{d,n} + \omega_{d,m})\sin(\omega_{d,n} + \omega_{d,m})t_2 - (\omega_n\zeta_n + \omega_m\zeta_m)\cos(\omega_{d,n} + \omega_{d,m})t_2}{2\{(\omega_n\zeta_n + \omega_m\zeta_m)^2 + (\omega_{d,n} + \omega_{d,m})^2\}}$$

Another integral needed throughout the text is

$$C_{nm}(x_1, x_2) = \int_{x_1}^{x_2} dx\, \phi_n(x)\phi_m(x)$$

where $\phi_n(x) = \sin n\pi x \qquad n = 1, 2, 3, \ldots$

The solution is

$$C_{nm}(x_1, x_2) = \frac{\sin(n-m)\pi x_2 - \sin(n-m)\pi x_1}{2\pi(n-m)} - \frac{\sin(n+m)\pi x_2 - \sin(n+m)\pi x_1}{2\pi(n+m)} \qquad n \neq m$$

$$= \frac{1}{2}(x_2 - x_1) - \frac{1}{4n\pi}(\sin 2n\pi x_2 - \sin 2n\pi x_1) \qquad n = m$$